Title:

Transcriptomic analysis of the C3-CAM transition in Cistanthe longiscapa, a drought tolerant plant in the Atacama Desert

Authors:

P. G. Ossa[1,2,3], A. A. Moreno[1], D. Orellana[4], M. Toro[1], T. Carrasco-Valenzuela[1], A. Riveros[1,2], C. C. Meneses[2,5,6,7], R. Nilo-Poyanco[8], A. Orellana[1,2]

Addresses:

1. Centro de Biotecnología Vegetal, Facultad de Ciencias de la Vida, Universidad Andrés Bello, República 330, Santiago, RM, 8370146, Chile.
2. Fondo de Desarrollo de Areas Prioritarias, Center for Genome Regulation, 8370415 Santiago, Chile.
3. Escuela de Veterinaria, Facultad de Ciencias, Universidad Mayor, Camino La Pirámide 5750, Huechuraba, Santiago, Chile.
4. Facultad de Ingeniería y Ciencias, Universidad Adolfo Ibañez. Av Diagonal Las Torres 2640, Peñalolén, Santiago, Chile.
5. Departamento de Fruticultura y Enología, Facultad de Agronomía e Ingeniería Forestal, Pontificia Universidad Católica de Chile, Santiago, 7820436, Chile.
6. Departamento de Genética Molecular y Microbiología, Facultad de Ciencias Biológicas, Pontificia Universidad Católica de Chile, Santiago, 8331150, Chile.
7. ANID - Millennium Science Initiative Program - Millennium Nucleus for the Development of Super Adaptable Plants (MN-SAP), Santiago, Chile.
8. Escuela de Biotecnología, Facultad de Ciencias, Universidad Mayor, Camino La Pirámide 5750, Huechuraba, Santiago, Chile.

Authors of correspondence:

Paulina G. Ossa

pgossa@bio.puc.cl

Ricardo Nilo-Poyanco

ricardo.nilo@umayor.cl

short running head:

Molecular basis of the C3-CAM in *C. longiscapa*

Abstract

One of the most outstanding plant species during the blooming of the Atacama Desert is the annual plant *Cistanthe longiscapa*. This plant can perform CAM photosynthesis, but the ecophysiological and molecular mechanisms that this plant uses to withstand the extreme conditions it inhabits in the field are unknown.

Morphological and ecophysiological traits were studied and leaf samples at dawn/dusk times were collected from three sites distributed across an increasing south to north arid gradient, to evaluate CAM expression and transcriptomic differences, and search for links between photosynthetic path and abiotic response.

Plants from the different sites presented significant differences in nocturnal leaf acid accumulation, isotopic carbon ratio ($\delta^{13}C$), succulence and other four traits that clearly indicated a spectrum of CAM photosynthesis intensity that correlated with aridity intensity. The differential gene expression analysis among Dawn vs Dusk between sampling sites showed higher gene expression in the arid northern site (3991 v/s 2293) with activation of regulatory processes associated with abscisic acid and circadian rhythm.

The analysis highlights clear ecophysiological differences and the requirement of a strong rewiring of the gene expression to allow a transition from a weak into a strong CAM in *C. longiscapa*.

Keywords: Abiotic Stress, Atacama Desert, CAM photosynthesis, *Cistanthe longiscapa*, C3-CAM spectrum, Drought, δ13C values, RNA-seq.

Introduction

In the upcoming years, it is expected that temperatures and drought periods will intensify due to climate change, affecting biodiversity at all levels (Feng and Fu, 2013; Schlaepfer *et al*., 2017), with terrestrial plants particularly exposed to these stressful environmental factors (Feng and Fu, 2013; Parmesan and Hanley, 2015; Schlaepfer *et al*., 2017). Plants can sense environmental changes rapidly and evolve morphological, physiological, and molecular adaptations to face them (Dussarrat *et al*., 2018). However, the mechanisms underlying these responses are still unknown, making it difficult to build any prediction model on how plants will face the aforementioned challenges. In times of a fast-growing human population (Gerland *et al*., 2014), uncovering these mechanisms is essential for a sustainable agricultural development, and a relevant input to engineer more resistant crops for a warmer and drier world (Borland *et al*., 2014; Borland *et al*., 2015; DePaoli *et al*., 2014; Yang *et al*., 2015).

Photosynthesis is an essential plant metabolic process, where atmospheric CO_2 is fixed into carbohydrates in a carbon cycle by RUBISCO, using the sun's energy and water. However, this process is affected by drought and elevated temperatures (Perdomo *et al*., 2017). Under arid conditions, plants face a limited water income, which is countered by an active reduction of stomata opening. This strategy enables the plant to lose less water through transpiration, a trade-off that can be costly by limiting CO_2 supply to photosynthesis (Bräutigam *et al*., 2017), and affecting the affinity of RUBISCO for CO_2 instead of O_2. To deal with this problem, some plants have evolved, together with adaptive morphological traits, CO_2-concentrating mechanisms that can be coupled to carbon fixation in the Calvin-Benson cycle (Raven and Beardall, 2016; Raven *et al*., 2017). Crassulacean acid metabolism (CAM) is a CO_2-concentrating mechanism remarkable for its high water-use efficiency (WUE) relative to C3 and C4 photosynthesis (Borland *et al*., 2009; Cushman *et al*., 2015). To reduce water loss, CAM plants fix CO_2 during the night by the action of the enzyme phosphoenolpyruvate carboxylase (PEPC), generating organic acids (mainly malate) that are stored in the vacuole. During the day, the night accumulated organic acids are decarboxylated and CO_2 is concentrated around RUBISCO to be fixed, entering the

Calvin-Benson cycle (C3 photosynthesis) to form carbohydrates, also reducing photorespiration, which can have a detrimental effect over photosynthesis (Pereira *et al*., 2021). Given this temporal separation, CAM plants can achieve high WUE compared to C3 and C4 plants (Wai *et al*., 2019).

CAM is a remarkable example of convergent evolution of a complex trait that has evolved independently multiple times in about 6% of species and at least 37 plant families (Winter *et al*., 2020). Different types of CAM have been described (Messerschmid *et al*., 2021; Winter and Smith, 2022), for instance, in obligate CAM plants, like most cacti, carbon is fixed constitutively at night in contrast to facultative CAM plants, where nocturnal fixation is induced by drought, salt stress or ontogeny (Winter K., 2019; Schiller and Bräutigam, 2021). In CAM cycling plants, carbon is fixed nocturnally from recycled respiratory CO_2, and during the day with C3 photosynthesis (Schiller and Bräutigam, 2021). CAM idling plants also perform CAM cycling, but stomata are always closed (Sipes and Ting, 1985). CAM species can also be classified as strong (CO_2 night uptake >70%) or weak CAM (CO_2 night uptake < 33%, Pereira *et al*., 2021). Plants performing weak CAM supplement the low-level nocturnal CO_2 fixation with high daytime C3 photosynthesis carbon fixation (Winter K., 2019, Schiller and Bräutigam, 2021). These weak CAM states can be considered as intermediate steps within the evolutionary spectrum from C3 to CAM, or as the final evolutionary state for lineages where it might be advantageous (Hancock *et al*., 2019; Heyduk *et al*., 2019). On the other hand, depending on the route that takes malate decarboxylation during the day, two different CAM pathways can be distinguished (Holtum *et al*., 2005, Shameer *et al*., 2018): one is the malic enzyme route (CAM-ME), where malate is decarboxylated either in the cytosol by NADP-dependent malic enzyme (NADP-ME) or in the mitochondria by NAD-dependent malic enzyme (NAD-ME). These decarboxylations produce pyruvate and CO_2, where pyruvate is transported to the chloroplast and converted to PEP by the chloroplastic PEP dikinase (PPDK). The other pathway is the PEP carboxykinase (PEPCK) route (CAM-PEPCK), where malate is decarboxylated by PEPCK producing PEP in the cytosol, so these species do not rely on PPDK. In addition, based on the transitory sugar accumulated, there are species where PEP is transiently stored as starch in the chloroplast, like in *Kalanchoe* or *Mesembryanthemum*

crystallinum; and others where it is stored in the vacuole as soluble saccharides like sucrose, fructose or glucose (Holtum *et al*., 2005; Borland et al., 2016). These pathways diversity probably stems from the multiple evolutionary origins of CAM (Niechayev *et al*., 2019).

The evolutionary basis of CAM and its plasticity is sustained in the fact that all CAM genes exist in C3 species, with genetic changes centered on regulation, timing or abundance of transcripts, gene duplications and neofunctionalization (Heyduk *et al*., 2018, 2019). Changes in transcript abundance and regulation related to circadian rhythm have been proposed as the main source of changes related to CAM (Wai *et al*., 2019). Recently, changes in amino acid biosynthesis flux have also been suggested as a possible mechanism towards developing CAM photosynthesis (Bräutigam *et al*., 2017). In addition, genome-scale analyses of constitutive CAM plants suggest that time of day networks are phased to the evening compared to C3, whereas in drought induced CAM, core clock genes either change phase or amplitude, with novel CAM and stress specific cis-elements being responsible for rewired co-expression networks (Wai *et al*., 2019; Chen *et al*., 2020).

Plant species inhabiting deserts have been exposed to the so-called stressful environmental conditions for thousands of years. Many of them have developed morphological and physiological adaptations that enhance their photosynthetic performance and survival under extreme arid conditions (Gibson AC., 1998, Wang *et al*., 2019), including the evolution of CAM photosynthesis, CAM-C3 intermediate or C4 mechanisms (Heyduk *et al*., 2019, Wang *et al*., 2019, Folk *et al*., 2020). The Atacama Desert is one of the driest places on earth, with precipitations only occurring sporadically. When, every few years, thresholds on precipitation abundance and frequency are meet, the phenomenon known as the “blooming desert” emerge (Vidiella *et al*., 1999; Chávez *et al*., 2019; Araya *et al*., 2020; Holtum *et al*., 2021). *Cistanthe longiscapa* (Bernaud) Carolin ex Hershkovitz (Montiaceae) is an endemic annual plant and one of the most widespread and abundant plants within the blooming Atacama Desert events (Holtum *et al*., 2021). Previous reports based on leaf carbon isotope ratios suggest that some Chilean members of *Cistanthe* are in the C3-CAM intermediate spectrum (Arroyo *et al*., 1990; Palma and Mooney, 1998), with *C. longiscapa* representing

a weak constitutive CAM (Holtum *et al*., 2021). Studies in other genus of the family, such as *Calandrinia* in Australia, have shown that many of these annual succulent species can be CAM facultative (Winter and Holtum, 2011; Holtum *et al*., 2017). In this work, we aim to explore the changes in gene expression associated to the C3-CAM spectrum in *C. longiscapa*, proposing that the intensity of CAM will vary concomitant with the intensity of aridity to which plants are exposed in the Atacama Desert. To this end, we studied the field variation on ecophysiological traits and CAM photosynthesis in *C. longiscapa*, assembled a *de novo* transcriptome followed by an RNA-seq comparative study from samples taken at dawn and dusk from three sampling sites, to track the changes in CAM/C3 switches under field conditions. The strength of this study lies in that it is the first transcriptomic study of an Atacama Desert blooming plant focused to unveil the molecular basis of the C3-CAM photosynthesis under natural environment conditions.

Materials and Methods

Sampling and plant traits measurement

Cistanthe longiscapa has a rosette with basal succulent leaves and inflorescence branches with showy terminal purple flowers, despite the strong impact of tourism during the blooming desert, this species is currently not threatened (Squeo *et al*., 2008). The study was conducted at the Atacama Desert, with all the samples being collected in July 2015, at the beginning of the flowering season. The year 2015 was a particular one in terms of precipitation timing, abundance, intensity (Wilcox. *et al*., 2016), and flowering abundance. Three sampling locations were selected between the localities of Copiapó and Vallenar, where populations of *Cistanthe longiscapa* (Bernéoud) Carolin ex Hershkovitz grows in extensive prairies when the flowering desert occur: Site 1 (S1) was set at 27°38'02.4"S 70°27'46.8"W, S2 at 27°57'57.6"S 70°33'25.2"W and S3 at 28°25'12.0"S 70°43'12.0"W. S1 and S2 site soils are calcisols, whereas site S3 display regosols (Supplementary Figure 1, Harmonized World Soil Database (version 1.2), Fischer *et al*., 2008). In each sampling site, fully expanded mature leaves from 10 healthy flowering plants were sampled at the evening (7-8 PM, henceforth “dusk”) and at the next morning (7-8 AM, henceforth “dawn”) on the same individuals, to determine nocturnal tissue acidification and prepare RNA extractions

to cDNA library construction. Once sampled, all samples were immediately frozen in liquid nitrogen and transported to the laboratory in a Taylor-Wharton CXR500 dry shipper. Also, at dawn, leaves from the same plants were sampled to determine leaf mass per area (LMA), saturated water content (SWC), carbon isotope composition ($\delta^{13}C$ (‰)), the percentage of Carbon and Nitrogen (%C, %N) and photosynthetic pigments content (chlorophyll A, chlorophyll B, carotenoids).

For LMA and SWC determination (Ogburn and Edwards, 2012), 5 leaves were freshly weighed, scanned for area determination, saturated with distilled water until constant weight, and oven dried at 75ºC for 48-72 hours until reaching a constant weight. LMA was calculated as: Dry weight (g) / area (m^2); and SWC as: [(Saturated weight (g) – dry weight (g)) / dry weight (g)]. For carbon isotope ratios and carbon and nitrogen composition, five fully expanded mature leaves per plant were dried, pooled, grinded, and analyzed at the Laboratory of Biogeochemistry and Applied Stable Isotopes (LABASI, PUC, Santiago, Chile) with an isotope ratio mass spectrometer and calculated against the Pee Dee belemnite (PDB) standard following Farquhar *et al*. (1989) equation. For chlorophyll and carotenoids content, leaves were instantly frozen in liquid nitrogen in the field and kept at -80º C until the pigments were extracted with DMSO following the protocol and equations described by Wellburn (1994).

To estimate the degree of CAM photosynthesis, titratable acidity was measured with NAOH 0.01N (Keeley and Keeley, 1989) in leaves collected at dawn and dusk (10 plants per site). The accumulation was estimated as the difference between dawn and dusk and reported as nocturnal leaf acid accumulation. Significant differences for all measured traits were estimated using T-Test (for paired comparisons) or one-way ANOVA for each trait displayed. Principal component analysis (PCA) was used to evaluate correlations among traits. All the statistics were carried out in R (R Core Team, 2020).

RNA isolation and cDNA library construction

Total RNA was extracted using Spectrum Plant Total RNA Kit (Sigma Aldrich, USA) from all the samples. We prepare 12 cDNA libraries (3 individuals □ 2 sampling times (dawn and dusk) □ 2 localities) using the TruSeq RNA-seq library prep kit from Illumina

(Illumina, Inc., CA, USA) according to manufacturer's instructions. cDNA libraries (Table S1) were sequenced in two lanes (paired-end 150 bp set-up) using HiSeq2500 sequencer (Macrogen Inc., Korea). Sequence data were deposited in the NCBI Short Read Archive in SUB10469409.

De novo transcriptome assembly

Before the transcriptome assembly, FastQC was used to check reads raw quality. Raw reads were trimmed with the Trim Galore Cutadapt (Martin and Wang, 2011) wrapper using the paired and -q 25 option to conserve high quality reads quality. Overall quality was checked before assembly using MultiQC (Ewels *et al*., 2016). De novo assembly of high-quality contigs for *C. longiscapa* were performed using the Trinity package v2.5.0 (Haas *et al*., 2013) following the authors recommendations and with "min_contig_length 400" as additional parameter to avoid very short contigs. The assembled *de novo* transcriptome was optimized with the TransRate package (Smith-Unna *et al*., 2016) using the authors' parameters recommendations. We look deeper into the transcriptome for ultra-conserved proteins using BUSCO (Simão *et al*., 2015) and the plant database Embryophyta odb09.

Cistanthe longiscapa gene functional annotation

Gene functional annotation was performed using Mercator version 4 (Lohse *et al*., 2014) and EggNOG version 4.5.1 (Huerta-Cepas *et al*., 2016) to determine the best homologue from the model plant *Arabidopsis thaliana*. First, the predicted transcripts were converted into proteins using the Transcript decoder 2 tool from Cyverse (Joyce *et al*., 2017), using the universal genetic code and minimum protein length of 100 amino acids options. Transcript predicted proteins were next annotated using Mercator, using the following setting: TAIR release 10 database was used as reference, with a blast cut-off of 80 (default). The Mercator *A. thaliana* gene hits were annotated using the Thalemine (Krishnakumar *et al*., 2017) annotation. The same dataset was also assessed using EggNOG, using the following setting: DIAMOND for Mapping mode, Taxonomic Scope was adjusted automatically, Orthologs search was run using the "Restrict to one-to-one" mode, and Gene Ontology Evidence was run using the "Use experimental terms only" mode.

Principal component and differential gene expression analysis

To maximize differences, only RNAseq from individuals from the extreme populations (S1 and S3) were used for differential expression analysis. Principal Component Analysis (PCA) was carried out using the R package FactoMineR (Lê *et al.*, 2008). Differential expression analysis was performed for libraries from S1 and S3 between conditions (dawn and dusk), using the DESeq2 package (Love *et al.*, 2014). Counts data was pre-processed to keep genes with at least 1.0 counts per million (cpm) in at least 3 samples. To maximize the number of differentially expressed genes detected, while controlling the false discovery rate (FDR), the Bioconductor package Independent Hypothesis Weighting (IHW, Ignatiadis *et al.*, 2016) was used to determine the adjusted *p-value* on DESeq2. Volcano plots were generated using the ggplot2 R package whereas heatmaps were generated using the pheatmap R package.

Gene ontology and pathways enrichment analysis

Gene ontology (GO) annotation from the best *A. thaliana* homologues was retrieved from the PlantGSEA (Yi *et al.*, 2013) "A. thaliana GO gene sets", and transferred to the genes from *C. longiscapa*. Next, this mapping was used to generate a Gene Matrix Transposed (GMT) file, where each row maps a GO term to the genes from *C. longiscapa* which have this annotation. This GMT file was used to assess GO enrichment using the g:Profiler web server (Raudvere *et al.*, 2019). In order to better characterize the g:Profiler results, the enriched GO terms redundancy was removed using REVIGO (Supek *et al.*, 2011), with the following parameters: Allowed similarity: Small (0.5); GO categories associated to: P-values; GO term sizes database: *A. thaliana*; semantic similarity measure to use: SimRel. Next, all the GO terms displayed by REVIGO were further summarized using the mclust method available at the simplifyEnrichment R/Bioconductor package version 1.2.0.

Pathway's enrichment analysis was also performed using the g:Profiler web server, based on the in house generated ClongiscapaCyc PTOOLS v25.0 pathway-genome database GMT file (PGDB, Karp *et al.*, 2021), build using as input the annotation results generated by the e2p2v4 enzymes annotation tool (Schläpfer *et al.,* 2017).

Gene regulatory networks analysis

DESeq filtered and normalized counts transcripts (Supplementary File 1) were used for inferring and analyzing gene regulatory networks (GRNs) related to the S1 and S3 site plants, using the R package DIANE (Cassan *et al*., 2021). Known transcriptional regulators related to CAM photosynthesis were retrieved from the literature (Supplementary Table S1, Brilhaus *et al*., 2016, Amin *et al*., 2019, Maleckova *et al*., 2019, De La Harpe *et al*., 2020, Moseley *et al*., 2021). After inference of the networks and empirical p-values assessment of the regulator-gene pair weights, edges above an FDR of 0.05 were kept to generate the final networks (Cassan *et al*., 2021).

qPCR validation

We validated, by qPCR, some of the transcripts that were differentially expressed among libraries and were related to "CAM photosynthesis", "Circadian Rhythm" and "Abiotic Stress" in the same samples used to perform the RNA-Seq libraries. One microgram of total RNA was treated with 1µL of DNAse I, amplification grade (Thermo Fisher Scientific) according to the manufacturer's instructions. This DNA-free RNA was used as a template for first-strand cDNA synthesis with an oligo(dT) primer and SuperScript II (Thermo Fisher Scientific), according to the manufacturer's instructions. The primers described in Supplementary Table S2 were used to amplify PCR products from single-stranded cDNA. qPCR was performed using the Fast EvaGreen qPCR Master Mix kit (Biotum, CA, USA). Reactions contained 1 µL of 1:10 diluted cDNA in a total volume of 10 µL. The quantification and normalization procedures were done using the following equation (Vandesompele *et al*., 2002; Hellemans *et al*., 2007):

$$Relative\ Expression = \frac{(1 + E\ target)^{-\Delta Ct\ target}}{\sqrt{[(1 + E\ Norm1)^{-\Delta Ct\ Norm\ 1}]x\ [(1 + E\ Norm2)^{-\Delta Ct\ Norm\ 2}]}}$$

where E corresponds to the efficiency of amplification of target and reference genes, Ct is the threshold cycle, and Norm1 and Norm2 refer to the references or normalizer genes. We selected *ClClathrin* and *ClGAPDH* as normalizer genes.

301

Results

Cistanthe longiscapa sampling on the Atacama's Desert

C. longiscapa (Figure 1, upper and mid panels) extends its distribution between 25º to 31ºS, from coastal habitats up to 3,800 m of elevation in sandy soils (Hershkovitz, 1991), where mean annual precipitation modeled after Bioclim 2.0 (Fick and Hijmans, 2017) is less than 40 mm/yr (Figure 1, lower panel). This species is widely distributed in valleys and coastal plains during the blooms after rare winter rainfall in the Atacama Desert (Araya *et al*., 2020; Holtum *et al*., 2021). The flowering period usually extends between September and December (late winter to early summer). Plants were collected from three sites along the Atacama Desert environmental arid gradient (López *et al*., 2016), displaying differences in precipitation values (Figure 1, lower panel) and soil type (Supplementary Figure 1).

Ecophysiological leaf traits points to different photosynthetic processes between S1 and S3 plants

To determine whether plants from the different sites displayed different ecophysiological performance, seven parameters associated with CAM and photosynthesis were analyzed (Figure 2A, Supplementary Figure 2). To this end, nocturnal leaf acid accumulation, isotopic ratio (δ13C), photosynthetic pigments (Chla, Chlb, Carotenoids), Carbon to Nitrogen ratio (C/N), leaf mass per area (LMA) and succulence (SWC) were assessed in leaves from ten plants from each site. Regarding the nocturnal acid accumulation, the highest values were reached in the northern site (S1, Δ Acidity = 251.56 ± 43.79 meqH+/g) and the lowest in the southern site (S3, Δ Acidity = 108.18 ± 41.8 meqH+/g), covering a spectrum of CAM photosynthesis intensity from strong to weak towards the south. The isotopic ratio (δ13C) measured in leaves of *C. longiscapa* also supports this spectrum, ranging from -15.42 to -24.15 ‰, values indicative of strong to weak CAM or C3-CAM intermediate (Messerschmid *et al*., 2021). For instance, the average in plants from S1 support a strong CAM (δ13C = -17.5‰ ± 1.2) in this northern sampling site, whereas the mean value in plants from S2 and S3 are more in agreement with weak CAM or C3-CAM photosynthesis (S2 δ13C = -22.2‰ ± 1.1; S3 δ13C = -19.5‰ ± 1.1). Photosynthetic pigments (Chla/Chlb = 2.13 ± 0.35) and Total Chlorophyll/Carotenoids (Ctot/Car = 3.41 ±

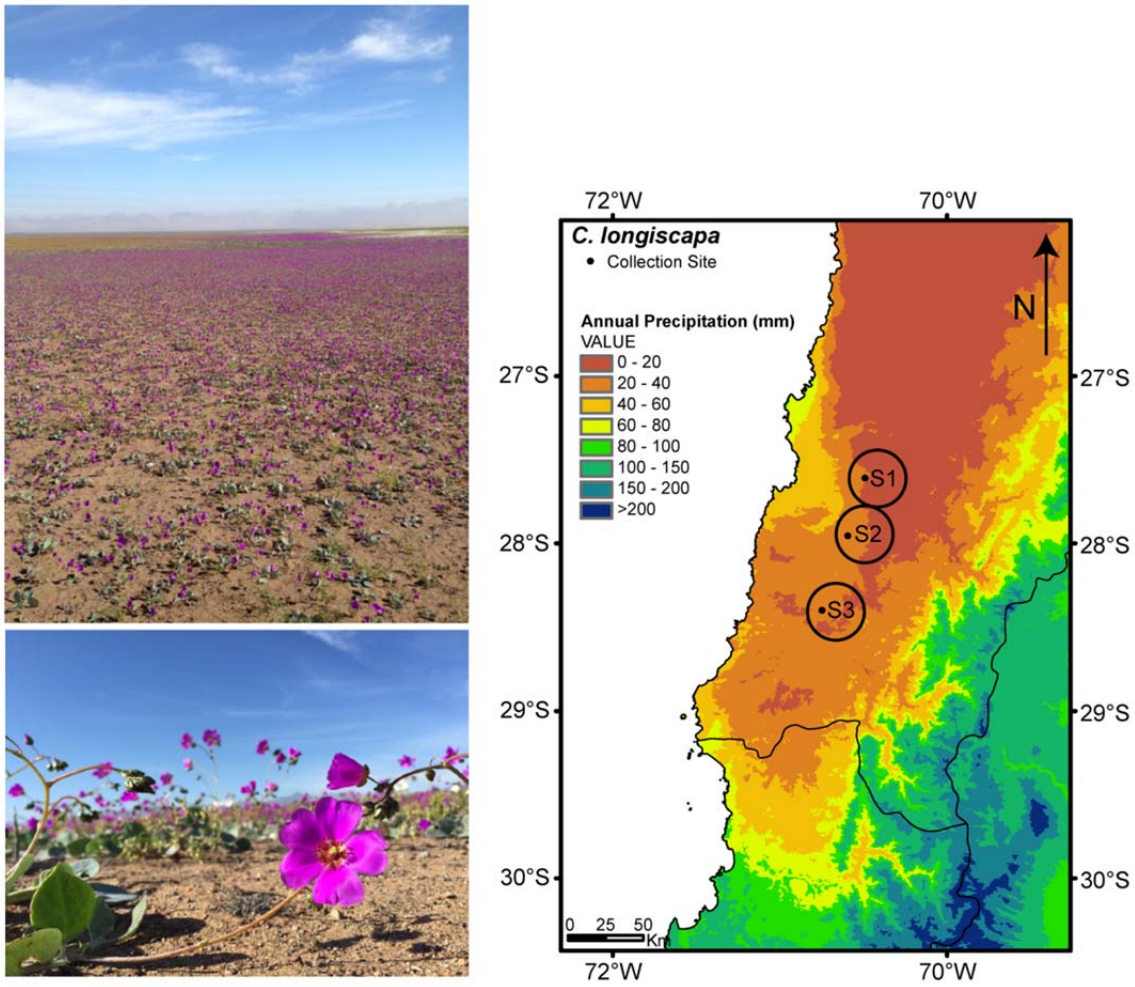

Figure 1. ***Cistanthe longiscapa*** **species and collection sites description.** The species model *Cistanthe longiscapa* can be seem as plants distributed as mantles of purple flowers in contrast with the arid Atacama Desert soil (upper and mid panels). A closer look allows the identification of a rosette with basal succulent leaves and inflorescence branches with terminal purple flowers. The geographic location of the study sites (S1, S2 and S3, lower panel) mapped against the average annual precipitation was obtained using Bioclim 2.0.

0.51) showed their lowest values in plants from S1, increasing towards S3, an opposite pattern compared to the nocturnal leaf acidification. Plants from the S1 site had the lowest leaf mass per area (131.35 ± 28.76), whereas the highest value for this parameter was in plants from S3 (170.84 ± 23.94). Regarding the Carbon to Nitrogen ratio, the highest value was found in plants from S1 (17.88 ± 2.13), whereas the lowest level was found in plants from S3 (12.55 ± 2.63). Finally, succulence (SWC) was higher in leaves from plants from the S1 compared to S2 and S3 sites.

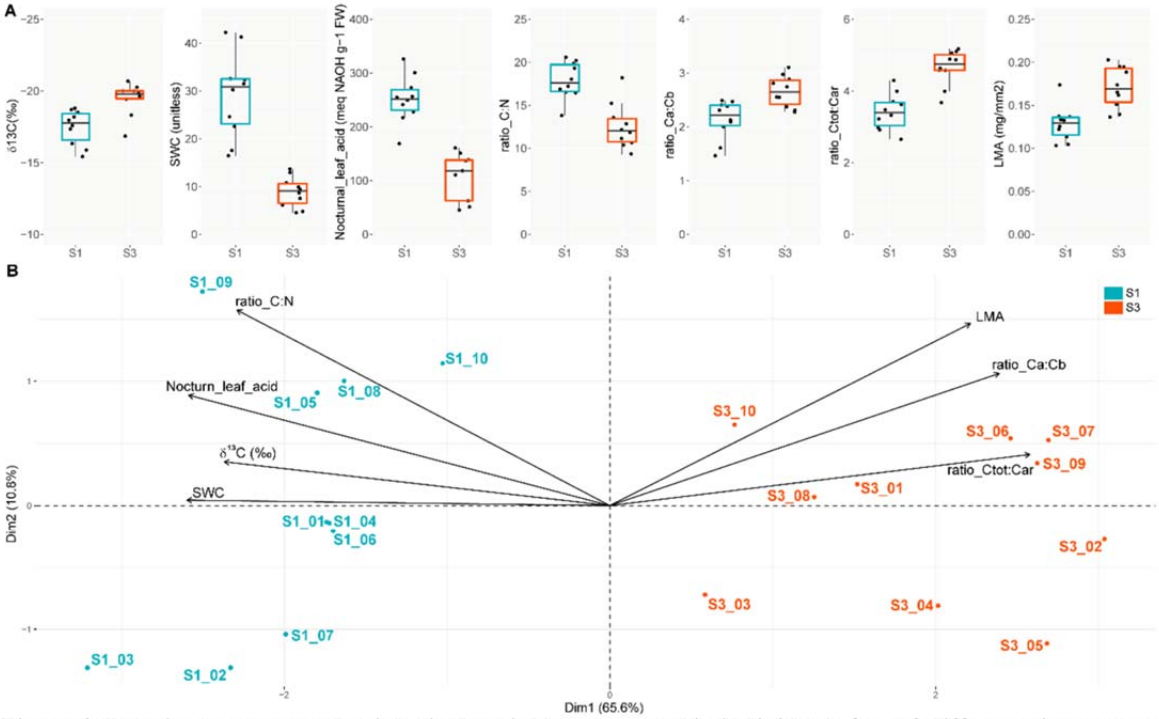

Figure 2. Relation among ecophysiological variables measured in individuals from 2 different sites across the Atacama Desert. Differences among sites S1 and S3 plants, in terms of nocturnal acid accumulation (Nocturnal_leaf_acid), isotopic carbon ratio ($\delta^{13}C$), leaf mass per area (LMA), succulence (SWC), total Chlorophyll/Carotenoids (ratio_Ctot:Car), Carbon to Nitrogen ratio (ratio_C:N) and photosynthetic pigments ratio (ratio_Chla:Chlb), were assessed (**A**). Principal component analysis using the data from these 7 traits allowed segregating and correlating the sampling sites with the different ecophysiological variables (**B**). TTtest, was used to assess the differences between sites S1 and S3 plants. All comparisons p-values were smaller than 0.005. N = 10.

To evaluate if the ecophysiological variations observed among the plants from the different sites replicate the geographic samples distribution, we performed a PCA analysis (Figure 2B). We observed that some variables strongly explain the segregation among geographic sampling sites. For example, the three best explanatory traits for CAM, δ13C, nocturnal leaf acidity accumulation and succulence (SWC) were correlated with Dim 1 (which accounted for 48.4% of the variance) and S1 site, segregating those samples from the other two sites. Leaf mass per area (LMA) and photosynthetic pigments (ratio Chla/Chlb and Ctot/Car) were correlated with Dim 1 in the opposite direction, and with S3 samples, explaining their segregation towards the other extreme of the Dim1 axis. These results suggest that *C. longiscapa* plants located in S1 and S3 sites performed different photosynthetic mechanisms.

352

353 **_De novo_ assembly of the _Cistanthe longiscapa_ transcriptome and differential gene**
354 **expression uncover different stress responses in plants from sites S1 and S3**

355 To get insights of the transcriptome repertoire of *C. longiscapa*, a de novo assembly was
356 carried out using RNA-seq reads from 12 libraries obtained from sites S1 and S3, collected
357 at dusk and dawn (Table 1), with a contig N50 of 1,128 bp. A total of 88,770 transcripts
358 were predicted, which could be translated into 43,241 non-redundant proteins. The
359 comparison against a set of highly conserved genes using BUSCO resulted in 61% of
360 completed and 14% of fragmented genes, while 25% of the genes were missing. Close to
361 90% (88.8%) of the predicted proteins were associated to a homologous protein when using
362 in parallel Mercator (Lohse *et al*., 2014) and EggNOG (Huerta-Cepas *et al*., 2016) gene
363 annotation tools (Supplementary Table S3). When considering only the *A. thaliana* best
364 homologues, annotated by Mercator, 32,886 transcripts (76.1%) were covered, with a one-
365 to-one relationship for 15.5% of these transcripts.

366

367 Principal component analysis of the RNAseq sample libraries clearly shows that the first
368 dimension discriminates by site of collection whereas the second discriminate by time of
369 sample collection (Figure 3A). Together, both dimensions accounted for 42.4% of the
370 variability in the transcriptome. In terms of data quantification, a total of 69,614 transcripts
371 of the *de novo C. longiscapa* transcriptome had expression values above 0. After the
372 removal of lowly expressed and low reproducibility genes, the gene set to be assessed
373 accounted for 35.3% of the original transcriptome (Supplementary Table S4,
374 Supplementary File 1). Genes with differential gene expression added up to 3,991 when
375 comparing dawn versus dusk at S1, and 2,564 at S3 (Figure 3B and C), with both sites
376 predominantly displaying higher gene expression levels at dawn (Figure 3D). At S1, the
377 dawn/dusk ratio was 2.3 (2771/1220 transcripts), whereas at S3 the ratio was 1.4
378 (1491/1073 transcripts). Regarding the genes that were more expressed at dawn in both
379 sites, close to 24% were shared (822 transcripts), whereas genes that were more expressed
380 at dusk in both sites were close to 18% (343 transcripts, Figure 3D).

381

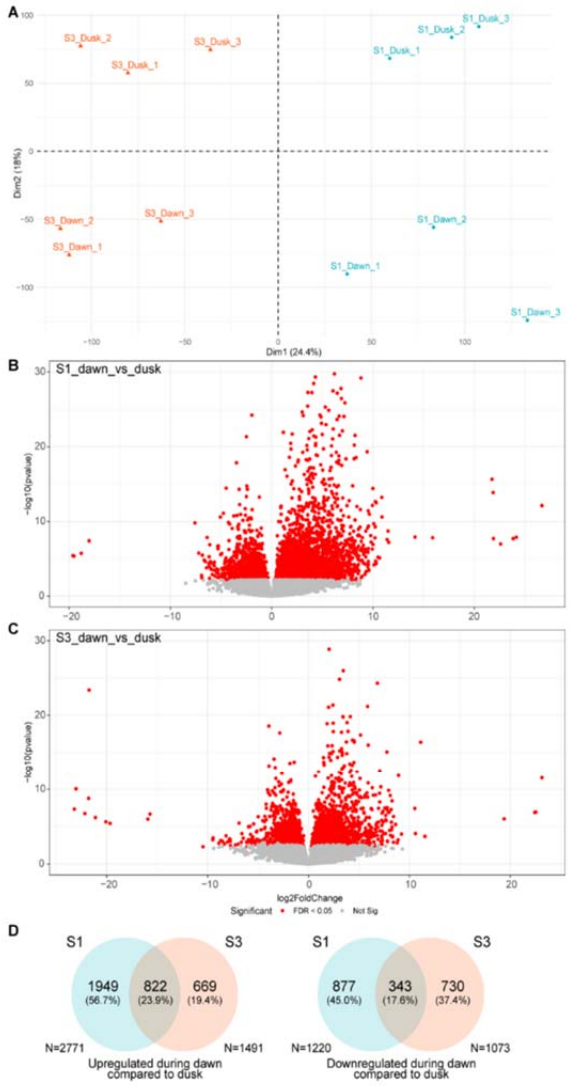

Figure 3. Relation *Cistanthe longiscapa* field data transcriptome analysis. Data from the *de novo* transcriptome from S1 and S3 plants, collected at dawn and dusk, was characterized by means of principal component analysis (**A**). The first dimension (PC1) split the data from sites S1 and S3, whereas PC2 split the data into dawn and dusk samples. Replicates, as expected, clustered together. The number and magnitude of transcripts significantly up or down-regulated at dawn compared to dusk are depicted as volcano-plots (**B**). At both S1 and S3 sites, most transcripts were upregulated at dawn, with the Site S1 displaying the higher number of transcripts differentially expressed. The maximum rates of change in both sites are similar, as can be seen by the units of the log2FoldChange X axis. In terms of similarities, sites S1 and S3 displayed 23.9% of the genes with similar up-regulation and 17.6% with similar downregulation at dawn (**C**).

382 Functional enrichment analysis of this data was performed using the Gene Ontology (GO)
383 annotation (Figure 4A; Supplementary Table S5) and MetaCyc pathways (Figure 4B). GO-

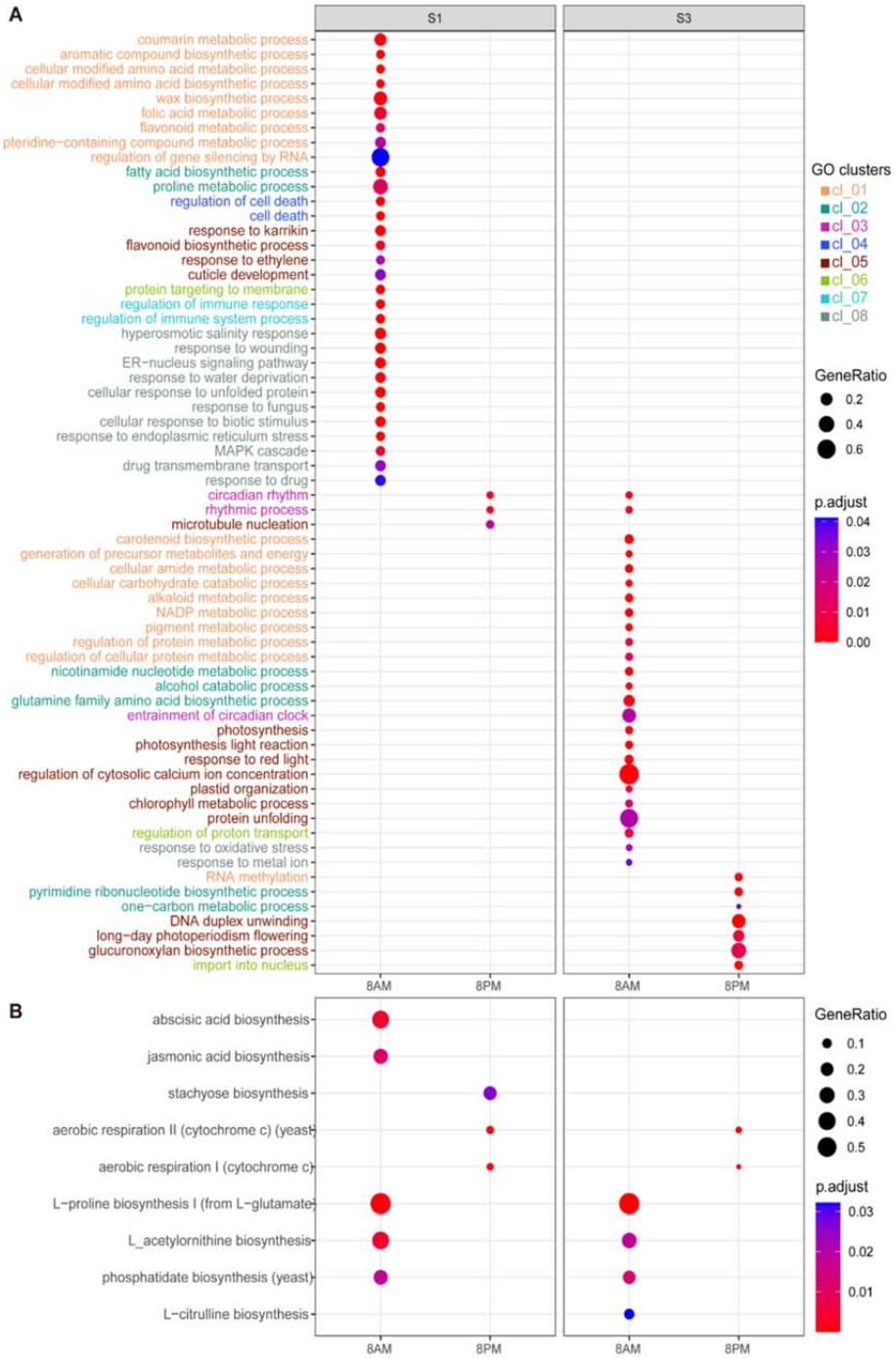

Figure 4. Functional enrichment analysis of genes upregulated at dawn or dusk in sites S1 and S3. The ratio and significance of GO (**A**) and MetaCyc pathways (**B**) of genes enriched at sites S1 and S3 at 8AM (up-regulated at dawn) and 8PM (up-regulated at dusk) are shown as dotplots. GO biological process (BP) terms were further grouped in 8 clusters according to their semantic similarity (Methods).

384 based analysis allowed the identification of 64 processes enriched in some of the four
385 conditions assessed. By using the corresponding semantic similarity matrix of these 64 GO

terms, we further grouped them in 8 clusters (Supplementary Figure 3). Clusters 1, 2 and 6 were similarly represented in both sites, whereas cluster 3 displayed an opposite pattern for each site, being related to circadian processes. Cluster 4, related to cell death, was only associated with S1 plants at dawn. Cluster 5 was more diverse and included GO processes related to photosynthesis associated with genes with higher expression at dawn at the site S3. Clusters 7 and 8 were related to abiotic stress, being preferentially associated to the transcripts with higher expression at dawn at the site S1.

In terms of pathways, abscisic acid biosynthesis displayed many genes with higher expression at S1 at dawn (Figure 5A), with genes involved in the biosynthesis of intermediate compounds and ABA transport also upregulated. Another set of pathways with a different expression profile between S1 and S3 were highlighted in Figure 5B. These pathways are key for regulating glutamine and glutamate accumulation and are also responsible for the biosynthesis of γ-aminobutyrate (GABA) which, as well as ABA, prompt plants to close stomata, a process that would be triggered at dawn in S1 site plants.

Gene regulatory network analysis identifies the gene network of S1 plants up regulated at dawn as the most complex

An analysis of 50 genes related to the control of the circadian clock (Supplementary Tables S6 and S7, Moseley *et al.*, 2021) showed that 28% of these genes displayed a higher expression at dawn, led by LHY1, which peaks in the morning, and the other 20% displayed a higher expression at dusk and were led by TOC1, which peaks in the evening (Schiller and Bräutigam, 2021). S3 plants displayed 20% of the 50 assessed circadian genes with an exclusive upregulation at dawn, as opposed to S1 plants, which displayed other 20% of the circadian clock genes with an exclusive upregulation at dusk.

Several of the genes involved in the control of the circadian clock have been recognized as key CAM transcriptional regulators (Brilhaus *et al.*, 2016, Amin *et al.*, 2019, Maleckova *et al.*, 2019, De La Harpe *et al.*, 2020, Moseley *et al.*, 2021). Therefore, we assessed the differences between S1 and S3 plants in terms of gene regulatory networks. The S1 GRN at dawn displayed more regulatory connections than any other GRN, with a link density of

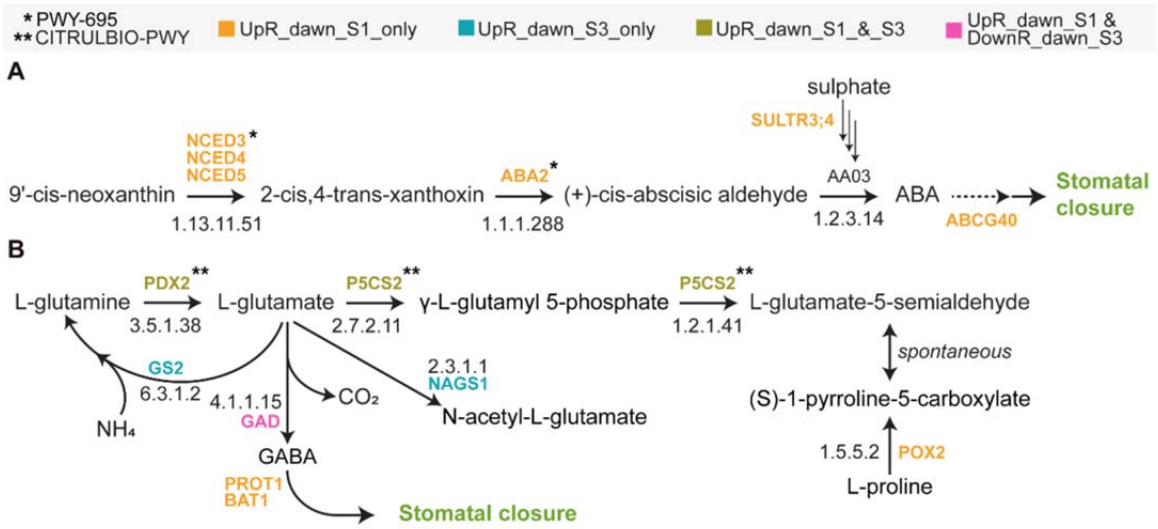

Figure 5. Pathways related to stomatal closure. The ABA biosynthesis pathway (**A**, PWY-695) included several genes up-regulated at dawn at the site S1 (stressed in bold-orange). We also pointed out genes that displayed the same pattern and that could be involved in ABA transport or in the biosynthesis important precursors for the enzymes of the pathway activity. The other pathways assessed were the L-citrulline biosynthesis (CITRULBIO-PWY), the acetylornithine biosynthesis (PWY-6922) and the proline biosynthesis I (PROSYN-PWY) pathways (**B**). Genes upregulated at dawn in both sites, or in S1 or in S3 are highlighted with different colors. Interestingly, the result of this regulation of these pathways would be the stomatal closure during the day in S1 site plants. ABA - abscisic acid; GABA - γ-aminobutyrate.

1.142 compared to 0.980 from the S3 GRN at dawn, the network with the second larger number of regulatory connections. Among the hubs found, the nuclear-encoded sigma factor 5 (SIGE), the *A. thaliana* homologue of AT2G44730, and the heat shock transcription factor A2 (HSFA2) were the top 3 (Table 2).

Community assessment based on GO enrichment analysis and normalized expression profiles (Supplementary Figure 4) also allowed to discriminate similarities and differences among the GRNs. For instance, the community number 3 in both S1 and S3 plants, at dusk, were similar in size, biological process GO enrichment and main hub genes. The community number 2 of the genes upregulated at dawn in S3 plants was, in turn, related to photosynthesis and displayed an expression change only in S3 plants. In addition, its main hub was the chloroplast-localized sigma factor SIGE, an essential factor in the nuclear

429 control of chloroplast function and its response to environmental stress (Mellenthin *et al*.,
430 2014, Zhang *et al*., 2020).
431
432 **Validation of Differential Expression of Genes using qPCR**
433 Based on the ecophysiological response and the enrichment on several GO terms associated
434 to photosynthesis on plants from the site S3 at dawn, we evaluated the transcript level of
435 genes associated to CAM metabolism such as PEPCK, PPDK, NADP-ME4
436 and RUBISCO activase (Figure 7). Among them, the transcript level of NADP-ME4
437 accumulates at dawn on plants from both sites whereas the transcripts of PEPCK, PPDK
438 and RUBISCO activase did not shown a particular pattern of expression between the
439 sampled sites, although PPDK transcript accumulation was higher on S1 samples. Given
440 the fact that GO terms associated to circadian rhythm displayed a contrasting temporal
441 pattern between sites S1 and S3 (Figure 4), the transcript level of two genes associated the
442 dark phase such as APRR1, Gigantea and one gene associated to the light phase like Late
443 Elongated Hypocotyl (LHY) were evaluated. As expected, the transcript levels of APRR1
444 and Gigantea reached their maximum at dusk, whereas the transcript of LHY reached their
445 maximum at dawn and the level of all transcripts were higher on samples from site S3
446 (Figure 7). Additionally, we evaluated the transcript levels of genes associated to ABA
447 biosynthesis, NCED3 and ABA2, considering the GO terms and MetaCyc pathways
448 enrichment in response to water and plant hormone signaling transduction (Figure 5). As
449 shown on Figure 7, the transcript level of NCED3 was higher on samples from S1 at dawn
450 whereas the transcript of ABA2 exhibited similar levels at dawn and dusk at each sampled
451 site, but with a slightly higher amount on S1 samples.
452
453

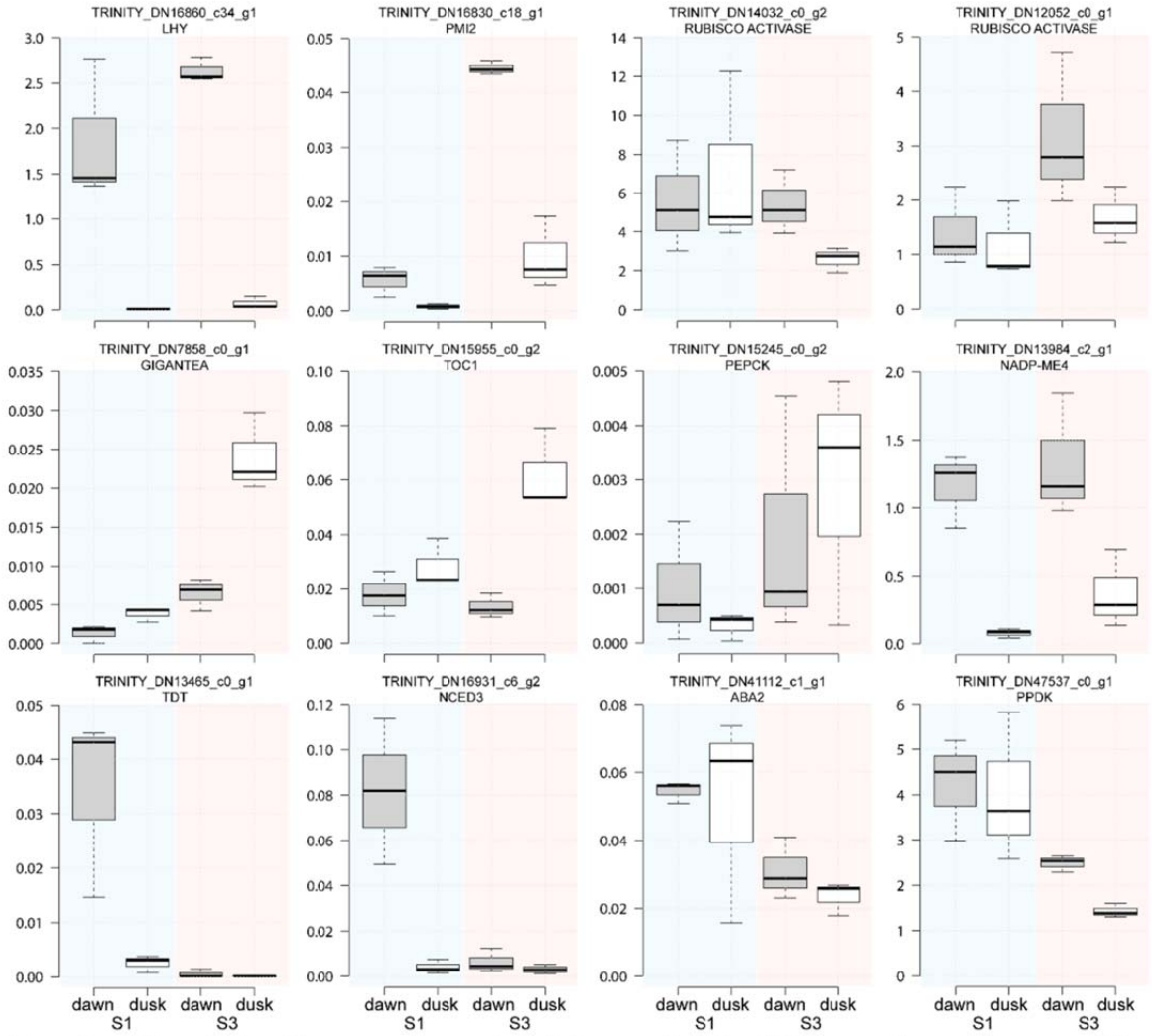

Figure 7. qPCR analysis of key genes expression at dawn and dusk. qPCR was performed for some of the transcripts that were related to "CAM photosynthesis", "Circadian Rhythm" and "Abiotic Stress" in the same samples used to perform the RNA-Seq libraries. The primers used are described in **Supplementary Table S2**.

Discussion

The Atacama Desert is a strongly arid environment, with a trend of aridity intensification towards the northern hyperarid core, particularly between the latitudes 30º and 25º, which enclose our sample sites (Figure 1, López *et al.*, 2016). The stochastic and rare rain-driven Atacama Desert blooming episodes can generate spatially isolated plant communities that remain separated during the intervening dry periods (Holtum *et al.*, 2021), providing a well-suited condition for functional traits intra-specific divergence according to the microenvironments the species are exposed to. Studying intra-specific variation can help understand evolutionary adaptations to environmental change and the

463 plants stress response (May *et al*., 2017). In this study evaluated intra-specific functional
464 traits from the annual plant *Cistanthe longiscapa*, a conspicuous member of the Family
465 Montiaceae, that grows during the "blooming desert" events. Plants located at different
466 desert landscapes (Figure 1 and Supplementary Figure 1) were ecophysiologically and
467 genetically characterized, which allowed us to detect different levels of CAM
468 photosynthesis in *C. longiscapa* plants from different sites. Focusing on the transitional
469 phases II (dawn) and IV (dusk) of the four-phase diurnal CAM cycle (Osmond CB, 1978),
470 we were able to capture transcriptional information from key processes for the plant
471 response to the environment, such as plant photorespiration, ABA and GABA biosynthesis
472 and circadian regulation, which could help understanding the molecular basis for the
473 metabolic flexibility shown between *C. longiscapa* plants inhabiting environments with
474 differences in aridity (Winter K, 2019).
475
476 CAM plants can be characterized by displaying a nocturnal acidification, a feature not
477 found in C3 plants (Winter and Smith, 2022). In this study we were able to detect different
478 levels of nocturnal leaf acidification in *C. longiscapa* plants collected from different sites
479 and to associate these differences with the development of an abiotic stress response. These
480 variations in acidity correlate with differences in δ13C contents, especially between the
481 most northern (S1) and southern (S3) collection sites (Figure 2), pointing to a constitutive
482 CAM in this species (Holtum *et al*., 2021), but with an environmentally sensitive CAM
483 modulation (Winter K., 2019, Schweiger *et al*., 2021). In addition to the differences of
484 δ13C and nocturnal titratable acid accumulation between S1 and S3 sites, our
485 ecophysiological results disclose higher chlorophyll a/b and chlorophyll/carotenoids ratios
486 in S3 plants, which could represent positive adaptive values of plants performing
487 photosynthesis under high light stress conditions (Gori *et al*., 2021). Differential expression
488 of genes related to photosynthesis and photorespiration at S3 also support the C3 diurnal
489 unfolding in S3 plants (Figure 4A). These results are remarkable because they show that *C.*
490 *longiscapa* is a species capable to live under extreme conditions of water scarcity by using
491 a resource conservative strategy such as CAM, that could be switched to a CAM-C3
492 resource expenditure strategy in response to almost imperceptible changes in arid
493 conditions that would provide a more amenable environment (Pereira and Cushman, 2019).

494

495 Other leaf functional trait analyzed was "Leaf mass per area" (LMA), that is the ratio
496 between leaf dry mass and leaf area. This trait would account for carbon and nutrients that
497 are invested in a certain area of light-intercepting foliage, reflecting the leaf-level cost of
498 light interception (Poorter *et al*., 2009), that is, high structural investment, lower mesophyll
499 conductance. In a strictly C3 plant we would have expected lower LMA values associated
500 with higher C3 photosynthesis performance but our results showed that plants from S1 have
501 the lowest LMA values, where carbon isotopic and leaf acidity values were indicatives of
502 more CAM and lesser C3 photosynthesis performance. This counterintuitive pattern can be
503 explained when we broke down LMA into leaf volume to area ratio (LVA, mL m-2) and
504 leaf density (LD, g mL-2) (De la Riva *et al*., 2016). Because of the presence of large
505 volumes of water-storage cells in succulents, LVA is over 10 times higher in succulent than
506 in non-succulent species, driven the variations in LMA in this kind of plants (Nielsen *et al*.,
507 1997). The negative correlation between LMA and succulence in our dataset (Figure 2)
508 corroborate this rationale, indicating that the observed variaton trend in LMA within these
509 plants is due to variation in water storage rather than structural investment. In small annual
510 plants, such as *C. longiscapa*, succulent leaves would represent single-use water stores
511 designed to extend the growing season into the portion of the year where resources such as
512 water become scarce (Males J., 2017). If the variation in LMA is due to LVA rather than
513 LD, it is expected that Carbon content remains relatively constant among sites. In effect,
514 C:N ratio remains constant in S1 and showed a sharply decreased in S3 (Supplementary
515 Fig. S2).
516
517 CAM nocturnal carbon uptake is made possible by the inverse stomatal behavior compared
518 to C3 plants, meaning stomatal opening at night and closure during all or part of the day,
519 leading to reduced water loss and improved water-use efficiency. Stomatal aperture is
520 regulated by diverse environmental signals, such as light and CO_2, as well as by internal
521 plant signals, such as abscisic acid (ABA) (Schiller and Bräutigam, 2021). Pathway-
522 enrichment analysis indicates that S1 plants display an enrichment in ABA and jasmonic
523 acid (JA) biosynthesis pathways (Figure 4B). ABA signaling can be induced by drought,
524 followed by stomatal closing to prevent water loss (Schiller and Bräutigam, 2021).

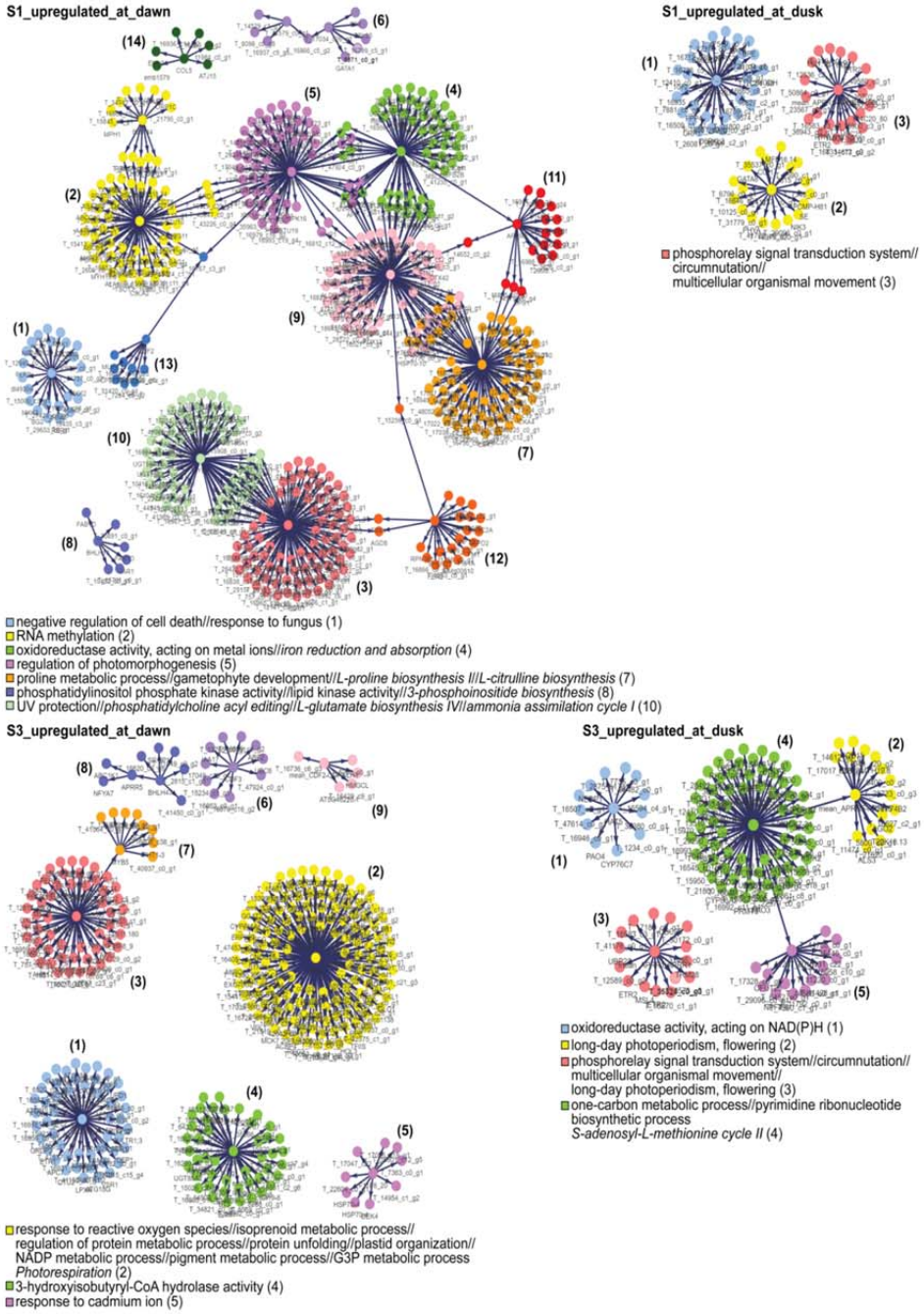

Figure 6. Gene regulatory networks associated to the expression profiles of S1 and S3 plants at dawn and dusk. GRNs were generated using the genes expression profile from S1 and S3 plants, at dawn and dusk. S1 and S3 networks at dawn were composed by many more communities (topological modules) than at dusk. The results of the communities GO enrichment analysis are shown below each network, with colors and numbers for each community used as identifiers. Enriched pathways are also indicated in italics. GO terms and pathways associated to the same community annotation are separated by a doble slash (//). Notice that the community colors are not related to the genes they are composed of, they just allow discriminating then.

525 Therefore, ABA synthesis and transport to target sites would be particularly required for

plants performing CAM photosynthesis, such as S1 plants. Noteworthy, we also found that sulphate transport might be regulated (Figure 5A) to increment ABA levels, possibly by providing sulfur for cysteine biosynthesis, which can be used downstream by ABA3, a MoCo-sulfurylase required for activating AAO3, the last step in the ABA biosynthesis (Cao *et al*., 2014). Also regulating AAO3 would be one of the main hubs of the S1 plant genes upregulated at dawn, the NAC transcription factor 29 (NAC29, Figure 6). NAC29 is, in fact, a TF associated with cold and drought responses that would have shown a lineage-specific gene expansion in the *C. longiscapa* family, the Montiaceae (Wang *et al*., 2019).

Many signaling pathways, besides those related to ABA, can be involved in regulating stomatal opening under drought stress conditions (Askari-Khorsgani *et al*., 2018). When assessing the differences between plants from the S1 and S3 sites related to pathways involved in the metabolism of key metabolites for the plant nitrogen homeostasis such as glutamine and glutamate (Figure 5B), it is possible to foresee how plants from the S3 site could use the enzyme glutamine synthetase 2 (GS2) at dawn to recycle ammonia derived from photorespiration (Ferreira *et al*., 2019). S1 plants, in turn, would be using the enzyme glutamate decarboxylase (GAD) to generate CO_2 and GABA, a compound known to be involved in reducing stomatal opening, therefore improving water use efficiency and drought tolerance (Xu *et al*., 2021), as well as generating diurnal CO_2 (Carillo P., 2018) under conditions where atmospheric CO2 would be limiting. In summary, the differential accumulation of the metabolites ABA and GABA could have a key role in the CAM diurnal stomatal closure of S1 *C. longiscapa* plants.

The inversed temporal CO_2 fixation characteristic of the CAM photosynthesis is apparently correlated to changes in the plant circadian clock (Wai *et al*., 2019, Moseley *et al*., 2021, Schiller and Bräutigam, 2021). *Sedum album* plants performing C3 and CAM drought-induced photosynthesis displayed 12.9 and 18.6% of the assessed genes cycling in one condition or the other, with only 22% of the genes cycling in both conditions (Wai *et al*., 2019), highlighting the significative rewiring of the transcriptome in response to drought conditions. About 48% of the genes related to the control of the circadian clock assessed in this work displayed a conserved pattern in S1 and S3 plants. S3 plants displayed 20% of the

assessed circadian genes with an exclusive upregulation at dawn, compared to S1 plants. Among those were PHYB and CRY2 which, together, regulate the chromatin degree of compaction under low light conditions (Martínez-Garcia and Moreno-Romero, 2020), enabling the transcription of the genes located in the exposed euchromatin regions.

A fine temporal and spatial regulation of metabolites and gases flow is required in CAM to avoid futile cycles, to favor the proper metabolites storage and to overcome the obstacles imposed by the succulent CAM plants leaf architecture. However, there are still several transporters that are unknown and are key for a CAM plant operation (Winter and Smith, 2022). Among the many transporters with a differential expression at dawn in S1 plants, we found several clearly related to the CAM metabolism: Dicarboxylate transporter (DiT1) and an aluminum-activated malate transporter (ALMT1) could be involved in the export of malic acid from the vacuole at dawn (Wai *et al*., 2019, Ceusters *et al*., 2021).

Succulent tissues might be advantageous for CAM plants due to the possibility to maximize the acid- and water-storage capacity of its cells (Lim *et al*., 2020, Winter and Smith, 2022). *C. longiscapa* plants from the S1 site, who would be performing CAM metabolism, displayed on average 3 times larger succulency compared to site S3 plants (Supplementary Figure 1). However, succulent leaves present tight packed water-rich cells, which represents an obstacle for CO_2 diffusion due to the lower diffusion speed of this gas in water compared to air (Schiller and Bräutigam, 2021). Aquaporins have been identified as facilitators of CO_2 diffusion across membranes (Gago *et al*., 2020), and therefore are good candidates for improving CO_2 diffusion in CAM succulent leaves. S1 plants displayed a higher level at dawn of two PIP1 proteins homologous to PIP1A and B, which could help the diffusion of CO_2 across the plant leaf tissues (Heckwolf *et al*., 2011).

Conclusions

The understanding of how a species can adjust its metabolism to perform C3 or CAM photosynthesis as a response to changes in its environment is key for CAM engineering in C3 crops, since it provides the opportunity to trigger CAM photosynthesis in periods of time when the plants are more susceptible to drought, and then return to a less energetically

588 expensive C3 mode. *C. longiscapa* is an annual "blooming desert" species that can perform
589 such transition as established in the present study, based on ecophysiological and
590 transcriptomic analysis of field samples.
591
592 *C. longiscapa* plants performing CAM photosynthesis would rely on the phytohormone
593 ABA and the signaling molecule GABA to reduce stomatal opening, and in more succulent
594 leaves to provide the proper leaf's vacuolar storage capacity required for performing CAM
595 (Töpfer et al., 2020). The temporal regulation of the processes that allow the switch
596 between a weak into a strong CAM photosynthesis would rely on the differential
597 expression of circadian clock genes during the late afternoon, and in a larger and more
598 elaborated gene regulatory network. In addition, our results reveal the importance of the
599 classic abiotic stress response associated to ABA into promote the shift between CAM
600 intensity and C3 photosynthesis. These results indicate that the transition from C3 into
601 CAM, even in plants that have evolved to do so, requires an important gene expression
602 rewiring, making the introgression of CAM into C3 crop plants a not so straightforward
603 process.
604
605 **Acknowledgments and Funding**
606 We specially thanks to A. Miquel, JP Parra-Rojas, for their valuable help in the lab and the
607 field work; to A. Miyasaka and D. Andrade for physiological instrumental facilitation and
608 technical support; to all members of the MUCILAB, especially S. Saez-Aguayo and A.
609 Largo-Gossens for their constant support, comments, and ideas. This work was funded by
610 FONDAP Center for Genome Regulation (CRG) 15090007 to A.O.; ANID-Fondecyt
611 Potsdoctorado 3510588 to P.O.; ANID-Fondecyt Iniciación 11150107 to R.N-P.; ANID-
612 Fondecyt Iniciación 11171175 to A.M; ANID-Fondecyt regular 1200804 to C.M.
613 The authors declare no competing financial interests.
614
615 **Author contributions**
616 P.O, C.M, A.M and A.O designed the study and analyses. P.O, D.O and M.T performed the
617 field collection and ecophysiological analyses. T.C and A.R assembled and quantified the
618 transcriptome. P.O, A.M and R.N-P performed data analysis. P.O, R.N-P performed

619 bioinformatics and statistical data analysis. A.O and C.M provided research opportunity
620 and funding. P.O, A.M, A.O and R.N-P wrote the manuscript.
621
622
623 **Tables**
624

Table 1: Assembly and annotation statistics for *Cistanthe longiscapa.*

Parameters	Values
Trinity genes	88770
GC (%)	42
Median contig (bp)	734
Average contig (bp)	990
Contig N10 (bp)	2926
Contig N20 (bp)	2191
Contig N30 (bp)	1731
Contig N40 (bp)	1397
Contig N50 (bp)	1128
Minimum length (bp)	401
Maximum length (bp)	402673
Annotated (*)	50280 (56.64%)
BUSCO (**)	61 (C); 14 (F); 25 (M)

(*) Aligned under non-redundant database (nr)
(**) Percentage of a total of 1440 genes, (C) Complete; (F) Fragmented; (M) Missing

625
626
627

628 **Table 2.** Gene Regulatory Network hubs associated to S1 and S3 plants differentially
629 expressed genes.

Table 2. Gene Regulatory Network hubs associated to S1 and S3 plants differentially expressed genes.

Network	Gene ID	Node Label	Degree	In-degree	Out-degree	Community	*Arabidopsis thaliana* homologue	Description
S1_upregulated_at_dawn	TRINITY_DN16963_c6_g2	T_16963_c6_g2	100	0	100	3	AT2G44730	Alcohol dehydrogenase transcription factor Myb/SANT-like family protein
	TRINITY_DN14945_c2_g1	HSFA2	94	1	93	9	AT2G26150	heat shock transcription factor A2
	mean_TRINITY_DN13374_c1_g1-TRINITY_DN16395_c0_g3-TRINITY_DN16860_c34_g1	mean_CDF2-CDF2-LHY	82	0	82	7	AT5G39660-AT5G39660-AT1G01060	cycling DOF factor 2-a; myb-related putative transcription factor involved in circadian rhythm
	TRINITY_DN28674_c0_g1	CDF3	69	0	69	5	AT3G47500	cycling DOF factor 3
	TRINITY_DN18858_c0_g1	MYB5	65	0	65	10	AT3G13540	myb domain protein 5
	TRINITY_DN16504_c1_g2	F11F8_20	63	2	61	4	AT3G09600	Homeodomain-like superfamily protein
	TRINITY_DN16381_c1_g1	NAC029	61	0	61	2	AT1G69490	NAC-like, activated by AP3/PI
	TRINITY_DN47711_c0_g1	CDF3	23	0	23	1	AT3G47500	cycling DOF factor 3
	TRINITY_DN16707_c10_g3	COL5	21	0	21	12	AT5G57660	CONSTANS-like 5
	TRINITY_DN15279_c1_g2	APRR5	18	1	10	11	AT5G24470	two-component response regulator-like protein
	TRINITY_DN16774_c0_g1	BZIP44	13	0	13	2	AT1G75390	basic leucine-zipper 44
	TRINITY_DN17777_c0_g1	CDF2	9	0	13	13	AT5G39660	cycling DOF factor 2
	TRINITY_DN10796_c0_g1	BHLH13	6	0	6	8	AT1G01260	basic helix-loop-helix (bHLH) DNA-binding superfamily protein
	TRINITY_DN17034_c26_g1	T_17034_c26_g1	6	0	6	6	AT2G40140	zinc finger (CCCH-type) family protein
	TRINITY_DN15561_c0_g2	COL5	6	0	6	14	AT5G57660	CONSTANS-like 5
	TRINITY_DN11579_c0_g1	T_11579_c0_g1	4	0	6	6	AT2G40140	zinc finger (CCCH-type) family protein
	TRINITY_DN24805_c0_g1	T_24805_c0_g1	3	3	0	4	NA	hypothetical protein
	TRINITY_DN16767_c3_g1	T_16767_c3_g1	3	3	0	13	NA	hypothetical protein
	TRINITY_DN40972_c0_g1	UVR8	3	0	3	4	AT5G63860	Regulator of chromosome condensation (RCC1) family protein
	TRINITY_DN17038_c7_g2	FRO6	3	3	0	5	AT5G49730	ferric reduction oxidase 6
	TRINITY_DN16728_c14_g1	AP2	3	3	0	5	AT4G36920	Integrase-type DNA-binding superfamily protein
	TRINITY_DN5238_c1_g1	TPR2	3	3	0	5	AT3G16830	TOPLESS-related 2
	TRINITY_DN43438_c0_g1	T_43438_c0_g1	3	3	0	5	NA	hypothetical protein
S3_upregulated_at_dawn	TRINITY_DN15226_c0_g1	SIGE	150	0	150	2	AT5G24120	sigma factor E
	TRINITY_DN16963_c6_g2	T_16963_c6_g2	55	0	55	3	AT2G44730	Alcohol dehydrogenase transcription factor Myb/SANT-like family protein
	TRINITY_DN28398_c0_g1	SCL13	50	0	50	1	AT4G17230	SCARECROW-like 13
	TRINITY_DN17777_c0_g1	CDF2	45	0	45	4	AT5G39660	cycling DOF factor 2
	TRINITY_DN28674_c0_g1	CDF3	10	0	10	6	AT3G47500	cycling DOF factor 3
	TRINITY_DN18858_c0_g1	MYB5	10	1	9	7	AT3G13540	myb domain protein 5
	TRINITY_DN16504_c1_g2	F11F8_20	9	0	9	5	AT3G09600	Homeodomain-like superfamily protein
	TRINITY_DN21874_c0_g1	BHLH47	6	0	6	8	AT3G47640	basic helix-loop-helix (bHLH) DNA-binding superfamily protein
	mean_TRINITY_DN13374_c1_g1-TRINITY_DN16395_c0_g3-TRINITY_DN16860_c34_g1	mean_CDF2-CDF2-LHY	5	0	5	9	AT5G39660-AT5G39660-AT1G01060	cycling DOF factor 2-a; myb-related putative transcription factor involved in circadian rhythm
	TRINITY_DN15279_c1_g2	APRR5	3	1	2	8	AT5G24470	two-component response regulator-like protein
S1_upregulated_at_dusk	TRINITY_DN16451_c1_g2	APRR3	30	0	30	1	AT5G60100	pseudo-response regulator 3
	mean_TRINITY_DN15955_c0_g1-TRINITY_DN15955_c0_g2-TRINITY_DN17074_c25_g1	mean_APRR1-APRR1-HSFC1	21	0	21	3	AT5G61380-AT5G61380-AT3G24520	CCT motif -containing response regulator protein (TOC1); heat shock transcription factor C1
	TRINITY_DN41237_c0_g1	T_41237_c0_g1	18	0	18	2	AT3G29270	RING/U-box superfamily protein
S3_upregulated_at_dusk	TRINITY_DN16451_c1_g2	APRR3	70	0	70	4	AT5G60100	pseudo-response regulator 3
	mean_TRINITY_DN16308_c3_g1-TRINITY_DN17033_c3_g2	mean_APRR5-APRR5	17	1	16	2	AT5G24470	two-component response regulator-like protein
	mean_TRINITY_DN15955_c0_g1-TRINITY_DN15955_c0_g2	mean_APRR1-APRR1	15	0	15	3	AT5G61380	CCT motif -containing response regulator protein (TOC1)
	TRINITY_DN41237_c0_g1	T_41237_c0_g1	15	1	14	5	AT3G29270	RING/U-box superfamily protein
	TRINITY_DN17072_c19_g2	HAT5	12	0	12	1	AT3G01470	homeobox 1

630
631

Figure Legends

Figure 1. *Cistanthe longiscapa* species and collection sites description. The species model *Cistanthe longiscapa* can be seem as plants distributed as mantles of purple flowers in contrast with the arid Atacama Desert soil (upper and mid panels). A closer look allows the identification of a rosette with basal succulent leaves and inflorescence branches with terminal purple flowers. The geographic location of the study sites (S1, S2 and S3, lower panel) mapped against the average annual precipitation was obtained using Bioclim 2.0.

Figure 2. Relation among ecophysiological variables measured in individuals from 2 different sites across the Atacama Desert. Differences among sites S1 and S3 plants, in terms of nocturnal acid accumulation (Nocturnal_leaf_acid), isotopic carbon ratio ($\delta^{13}C$), leaf mass per area (LMA), succulence (SWC), total Chlorophyll/Carotenoids (ratio_Ctot:Car), Carbon to Nitrogen ratio (ratio_C:N) and photosynthetic pigments ratio (ratio_Chla:Chlb), were assessed (**A**). Principal component analysis using the data from these 7 traits allowed segregating and correlating the sampling sites with the different ecophysiological variables (**B**). TTtest, was used to assess the differences between sites S1 and S3 plants. All comparisons p-values were smaller than 0.005. N = 10.

Figure 3. Relation *Cistanthe longiscapa* field data transcriptome analysis. Data from the *de novo* transcriptome from S1 and S3 plants, collected at dawn and dusk, was characterized by means of principal component analysis (**A**). The first dimension (PC1) split the data from sites S1 and S3, whereas PC2 split the data into dawn and dusk samples. Replicates, as expected, clustered together. The number and magnitude of transcripts significantly up or down-regulated at dawn compared to dusk are depicted as volcano-plots (**B**). At both S1 and S3 sites, most transcripts were upregulated at dawn, with the Site S1 displaying the higher number of transcripts differentially expressed. The maximum rates of change in both sites are similar, as can be seen by the units of the log2FoldChange X axis. In terms of similarities, sites S1 and S3 displayed 23.9% of the genes with similar up-regulation and 17.6% with similar downregulation at dawn (**C**).

Figure 4. Functional enrichment analysis of genes upregulated at dawn or dusk in sites S1 and S3. The ratio and significance of GO (**A**) and MetaCyc pathways (**B**) of genes enriched at sites S1 and S3 at 8AM (up-regulated at dawn) and 8PM (up-regulated at dusk) are shown as dotplots. GO biological process (BP) terms were further grouped in 8 clusters according to their semantic similarity (Methods).

Figure 5. Pathways related to stomatal closure. The ABA biosynthesis pathway (**A**, PWY-695) included several genes up-regulated at dawn at the site S1 (stressed in bold-orange). We also pointed out genes that displayed the same pattern and that could be involved in ABA transport or in the biosynthesis important precursors for the enzymes of the pathway activity. The other pathways assessed were the L-citrulline biosynthesis (CITRULBIO-PWY), the acetylornithine biosynthesis (PWY-6922) and the proline biosynthesis I (PROSYN-PWY) pathways (**B**). Genes upregulated at dawn in both sites, or in S1 or in S3 are highlighted with different colors. Interestingly, the result of this regulation of these pathways would be the stomatal closure during the day in S1 site plants. ABA - abscisic acid; GABA - γ-aminobutyrate.

Figure 6. Gene regulatory networks associated to the expression profiles of S1 and S3 plants at dawn and dusk. GRNs were generated using the genes expression profile from S1 and S3 plants, at dawn and dusk. S1 and S3 networks at dawn were composed by many more communities (topological modules) than at dusk. The results of the communities GO enrichment analysis are shown below each network, with colors and numbers for each community used as identifiers. Enriched pathways are also indicated in italics. GO terms and pathways associated to the same community annotation are separated by a doble slash (//). Notice that the community colors are not related to the genes they are composed of, they just allow discriminating then.

Figure 7. qPCR analysis of key genes expression at dawn and dusk. qPCR was performed for some of the transcripts that were related to "CAM photosynthesis", "Circadian Rhythm" and "Abiotic Stress" in the same samples used to perform the RNA-Seq libraries. The primers used are described in **Supplementary Table S2**.

694 **Supplemental Material**
695

696 **Fig. S1. Analysis of soil type at the selected samples collection sites.** The HWSD Viewer
697 from the Harmonized World Soil Database (version 1.2) was used to localize the sites the
698 selected samples collection sites and determine the type of soil they were associated to.
699 Arenosols are sandy soils featuring very weak or no soil development; Calcisols are soils
700 with accumulation of secondary calcium carbonates and Regosols are soils with very
701 limited soil development.
702

703 **Fig. S2. Statistical assessment of the differences between Sites S1, S2 and S3 plants**
704 **ecophysiological parameters.** Differences among sites S1, S2 and S3 plants, in terms of
705 nocturnal acid accumulation (Nocturnal_leaf_acid), isotopic carbon ratio ($\delta^{13}C$), leaf mass
706 per area (LMA); succulence (SWC); total Chlorophyll/Carotenoids (ratio_Ctot:Car);
707 Carbon to Nitrogen ratio (ratio_C:N) and photosynthetic pigments ratio (ratio_Chla:Chlb),
708 were assessed by means of ANOVA, for all analysis but SWC. For SWC, given the data
709 did not displayed homogeneity among samples, a Kruskal Wallis statistical test was
710 performed. N = 10 (A). A PCA was also performed using these samples (B).
711

712 **Fig. S3. GO data clustering.** GO terms acquired from REVIGO were further summarized
713 using the mclust method available at the simplifyEnrichment R/Bioconductor package
714 version 1.2.0.The eight clusters that summarize the 64 GO terms are shown at the right side
715 of the graph together with a similarity degree scale.
716

717 **Fig. S4. Normalized expression profiles from differentially expressed genes from S1**
718 **and S3 sites plants, at dawn and dusk.** Gene expression profiles associated to each
719 community (topological module) of the four GRNs assessed in this work are displayed.
720 Gene expression profiles are defined as the normalized counts (expression) divided by the
721 mean normalized counts across all conditions. S1D - S1 plants genes with higher
722 expression at dawn; S1N - S1 plants genes with higher expression at dusk; S3D - S3 plants
723 genes with higher expression at dawn; S3N - S3 plants genes with higher expression at
724 dusk.
725

Table S1: Data of putative CAM key gene expression regulators.

Table S2: qPCR primers description.

Table S3: *Cistanthe longiscapa* genes that were functionally annotated.

Table S4: Genes with a differential expression between dawn and dusk, for the S1 and S3 sites.

Table S5: Results from the GO and pathways analysis of the genes with a differential expression between dawn and dusk at the sites S1 and S3.

Table S6: Data of circadian clock genes assessed in this work.

Supplementary File 1: Filtered and normalized gene expression of the genes assessed for differential expression.

Parsed Citations

Amin AB, Rathnayake KN, Yim WC, Garcia TM, Wone B, Cushman JC, Wone BW. 2019. Crassulacean acid metabolism abiotic stress-responsive transcription factors: a potential genetic engineering approach for improving crop tolerance to abiotic stress. Frontiers in Plant Science 22: 10–129.
Google Scholar: Author Only Title Only Author and Title

Araya JP, González M, Cardinale M, Schnell S, Stoll A. 2020. Microbiome dynamics associated with the Atacama flowering desert. Frontiers in microbiology 22: 10–3160.
Google Scholar: Author Only Title Only Author and Title

Arroyo MK, Medina E, Ziegler H. 1990. Distribution and δ 13C values of Portulacaceae species of the high Andes in northern Chile. Botanica Acta 103: 291–5.
Google Scholar: Author Only Title Only Author and Title

Askari-Khorsgani O, Flores FB, Pessarakli M. 2018. Plant signaling pathways involved in stomatal movement under drought stress conditions. Adv Plants Agric Res 8: 290-297.
Google Scholar: Author Only Title Only Author and Title

Astorga-Eló M, Zhang Q, Larama G, Stoll A, Sadowsky MJ, Jorquera MA. 2020. Composition, predicted functions and co-occurrence networks of rhizobacterial communities impacting flowering desert events in the Atacama Desert, Chile. Frontiers in microbiology. 11: 571.
Google Scholar: Author Only Title Only Author and Title

Blondel VD, Guillaume JL, Lambiotte R, Lefebvre E. 2008. Fast unfolding of communities in large networks. Journal of statistical mechanics: theory and experiment 9:P10008.
Google Scholar: Author Only Title Only Author and Title

Borland AM, Griffiths H, Hartwell J, Smith JA. 2009. Exploiting the potential of plants with crassulacean acid metabolism for bioenergy production on marginal lands. Journal of Experimental Botany 60: 2879-96.
Google Scholar: Author Only Title Only Author and Title

Borland AM, Hartwell J, Weston DJ, Schlauch KA, Tschaplinski TJ, Tuskan GA, Yang X, Cushman JC. 2014. Engineering crassulacean acid metabolism to improve water-use efficiency. Trends in plant science 19:327–338.
Google Scholar: Author Only Title Only Author and Title

Borland AM, Wullschleger SD, Weston DJ, Hartwell J, Tuskan GA, Yang X, Cushman JC. 2015. Climate-resilient agroforestry: physiological responses to climate change and engineering of crassulacean acid metabolism (CAM) as a mitigation strategy. Plant, cell & environment 38: 1833–1849.
Google Scholar: Author Only Title Only Author and Title

Borland AM, Guo HB, Yang X, Cushman JC. 2016. Orchestration of carbohydrate processing for crassulacean acid metabolism. Current Opinion in Plant Biology 31:118-124.
Google Scholar: Author Only Title Only Author and Title

Bräutigam A, Schlüter U, Eisenhut M, Gowik U. On the evolutionary origin of CAM photosynthesis. Plant physiology. 2017 Jun;174(2):473-7.
Google Scholar: Author Only Title Only Author and Title

Brilhaus D, Bräutigam A, Mettler-Altmann T, Winter K, Weber AP. Reversible burst of transcriptional changes during induction of crassulacean acid metabolism in Talinum triangulare. Plant physiology. 2016 Jan;170(1):102-22.
Google Scholar: Author Only Title Only Author and Title

Cao MJ, Wang Z, Zhao Q, Mao JL, Speiser A, Wirtz M, Hell R, Zhu JK, Xiang CB. Sulfate availability affects ABA levels and germination response to ABA and salt stress in Arabidopsis thaliana. The Plant Journal. 2014 Feb;77(4):604-15.
Google Scholar: Author Only Title Only Author and Title

Carillo P. GABA shunt in durum wheat. Frontiers in Plant Science. 2018 Feb 2;9:100.

Cassan O, Lèbre S, Martin A. Inferring and analyzing gene regulatory networks from multi-factorial expression data: a complete and interactive suite. BMC genomics. 2021 Dec;22(1):1-5.
Google Scholar: Author Only Title Only Author and Title

Ceusters J, Van de Poel B. Ethylene exerts species-specific and age-dependent control of photosynthesis. Plant physiology. 2018 Apr;176(4):2601-12.
Google Scholar: Author Only Title Only Author and Title

Ceusters N, Borland AM, Ceusters J. How to resolve the enigma of diurnal malate remobilisation from the vacuole in plants with crassulacean acid metabolism? New Phytologist. 2021 Mar;229(6):3116-24.
Google Scholar: Author Only Title Only Author and Title

Chávez RO, Moreira-Muñoz A, Galleguillos M, Olea M, Aguayo J, Latín A, Aguilera-Betti I, Muñoz AA, Manríquez H. GIMMS NDVI time series reveal the extent, duration, and intensity of "blooming desert" events in the hyper-arid Atacama Desert, Northern Chile. International Journal of Applied Earth Observation and Geoinformation. 2019 Apr 1;76:193-203.

Chen Z, Zhao PX, Miao ZQ, Qi GF, Wang Z, Yuan Y, Ahmad N, Cao MJ, Hell R, Wirtz M, Xiang CB. SULTR3s function in chloroplast sulfate uptake and affect ABA biosynthesis and the stress response. Plant physiology. 2019 May;180(1):593-604.
Google Scholar: Author Only Title Only Author and Title

Chen LY, Xin Y, Wai CM, Liu J, Ming R. The role of cis-elements in the evolution of crassulacean acid metabolism photosynthesis. Horticulture research. 2020 Jan 1;7(1):1-8.

Cushman JC, Davis SC, Yang X, Borland AM. Development and use of bioenergy feedstocks for semi-arid and arid lands. Journal of Experimental Botany. 2015 Jul 1;66(14):4177-93.

De La Harpe M, Paris M, Hess J, Barfuss MH, Serrano-Serrano ML, Ghatak A, Chaturvedi P, Weckwerth W, Till W, Salamin N, Wai CM. Genomic footprints of repeated evolution of CAM photosynthesis in a Neotropical species radiation. Plant, Cell & Environment. 2020 Dec;43(12):2987-3001.
Google Scholar: Author Only Title Only Author and Title

De la Riva EG, Olmo M, Poorter H, Ubera JL, Villar R. Leaf mass per area (LMA) and its relationship with leaf structure and anatomy in 34 Mediterranean woody species along a water availability gradient. PloS one. 2016 Feb 11;11(2):e0148788.
Google Scholar: Author Only Title Only Author and Title

DePaoli HC, Borland AM, Tuskan GA, Cushman JC, Yang X. Synthetic biology as it relates to CAM photosynthesis: challenges and opportunities. Journal of Experimental Botany. 2014 Jul 1;65(13):3381-93.

Dussarrat T, Decros G, Díaz FP, Gibon Y, Latorre C, Rolin D, Gutiérrez RA, Pétriacq P. Another Tale from the Harsh World: How Plants Adapt to Extreme Environments. Annual Plant Reviews online. 2018 Feb 15:551-603.

Eisenhut M, Roell MS, Weber AP. Mechanistic understanding of photorespiration paves the way to a new green revolution. New Phytologist. 2019 Sep;223(4):1762-9.
Google Scholar: Author Only Title Only Author and Title

Ewels P, Magnusson M, Lundin S, Käller M. MultiQC: summarize analysis results for multiple tools and samples in a single report. Bioinformatics. 2016 Oct 1;32(19):3047-8.

Farquhar GD, Hubick KT, Condon AG, Richards RA. Carbon isotope fractionation and plant water-use efficiency. InStable isotopes in ecological research 1989 (pp. 21-40). Springer, New York, NY.

Feng S, Fu Q. Expansion of global drylands under a warming climate. Atmospheric Chemistry and Physics. 2013 Oct 14;13(19):10081-94.

Ferreira S, Moreira E, Amorim I, Santos C, Melo P. Arabidopsis thaliana mutants devoid of chloroplast glutamine synthetase (GS2) have non-lethal phenotype under photorespiratory conditions. Plant Physiology and Biochemistry. 2019 Nov 1;144:365-74.

Fick SE, Hijmans RJ. WorldClim 2: new 1-km spatial resolution climate surfaces for global land areas. International journal of climatology. 2017 Oct;37(12):4302-15.
Google Scholar: Author Only Title Only Author and Title

Fischer G, Nachtergaele F, Prieler S, van Velthuizen HT, Verelst L, Wiberg D. 2008. Global Agro-ecological Zones Assessment for Agriculture (GAEZ 2008). IIASA, Laxenburg, Austria and FAO, Rome, Italy.
Google Scholar: Author Only Title Only Author and Title

Folk RA, Siniscalchi CM, Soltis DE. Angiosperms at the edge: Extremity, diversity, and phylogeny. Plant, Cell & Environment. 2020 Dec;43(12):2871-93.
Google Scholar: Author Only Title Only Author and Title

Gago J, Daloso DM, Carriquí M, Nadal M, Morales M, Araújo WL, Nunes-Nesi A, Perera-Castro AV, Clemente-Moreno MJ, Flexas J. The photosynthesis game is in the" inter-play": mechanisms underlying CO2 diffusion in leaves. Environmental and Experimental Botany. 2020 Oct 1;178:104174.
Google Scholar: Author Only Title Only Author and Title

Gerland P, Raftery AE, Ševčíková H, Li N, Gu D, Spoorenberg T, Alkema L, Fosdick BK, Chunn J, Lalic N et al. World population stabilization unlikely this century. Science. 2014 Oct 10;346(6206):234-7.

Gibson AC. Photosynthetic organs of desert plants. Bioscience. 1998 Nov 1;48(11):911-20.

Gori A, Brunetti C, dos Santos Nascimento LB, Marino G, Guidi L, Ferrini F, Centritto M, Fini A, Tattini M. Photoprotective Role of Photosynthetic and Non-Photosynthetic Pigments in Phillyrea latifolia: Is Their "Antioxidant" Function Prominent in Leaves Exposed to Severe Summer Drought? International Journal of Molecular Sciences. 2021 Jan;22(15):8303.
Google Scholar: Author Only Title Only Author and Title

Guralnick LJ, Gilbert KE, Denio D, Antico N. The development of crassulacean acid metabolism (CAM) photosynthesis in cotyledons of the C4 species, Portulaca grandiflora (Portulacaceae). Plants. 2020 Jan;9(1):55.
Google Scholar: Author Only Title Only Author and Title

Hancock LP, Holtum JA, Edwards EJ. The evolution of CAM photosynthesis in Australian Calandrinia reveals lability in C3+ CAM phenotypes and a possible constraint to the evolution of strong CAM. Integrative and comparative biology. 2019 Sep 1;59(3):517-34.

Haas BJ, Papanicolaou A, Yassour M, Grabherr M, Blood PD, Bowden J, Couger MB, Eccles D, Li B, Lieber M, MacManes MD. De novo transcript sequence reconstruction from RNA-seq using the Trinity platform for reference generation and analysis. Nature protocols. 2013 Aug;8(8):1494-512.
Google Scholar: Author Only Title Only Author and Title

Heckwolf M, Pater D, Hanson DT, Kaldenhoff R. The Arabidopsis thaliana aquaporin AtPIP1; 2 is a physiologically relevant CO2 transport facilitator. The Plant Journal. 2011 Sep;67(5):795-804.
Google Scholar: Author Only Title Only Author and Title

Hedrich R, Sauer N, Neuhaus HE. Sugar transport across the plant vacuolar membrane: nature and regulation of carrier proteins. Current Opinion in Plant Biology. 2015 Jun 1;25:63-70.

Hellemans J, Mortier G, De Paepe A, Speleman F, Vandesompele J. qBase relative quantification framework and software for management and automated analysis of real-time quantitative PCR data. Genome biology. 2007 Feb;8(2):1-4.
Google Scholar: Author Only Title Only Author and Title

Heyduk K, Hwang M, Albert V, Silvera K, Lan T, Farr K, Chang TH, Chan MT, Winter K, Leebens-Mack J. Altered gene regulatory networks are associated with the transition from C3 to crassulacean acid metabolism in Erycina (Oncidiinae: Orchidaceae). Frontiers in plant science. 2019 Jan 28;9:2000.
Google Scholar: Author Only Title Only Author and Title

Heyduk K, Moreno-Villena JJ, Gilman IS, Christin PA, Edwards EJ. The genetics of convergent evolution: insights from plant photosynthesis. Nature Reviews Genetics. 2019 Aug;20(8):485-93.
Google Scholar: Author Only Title Only Author and Title

Holtum JA, Smith JA, Neuhaus HE. Intracellular transport and pathways of carbon flow in plants with crassulacean acid metabolism. Functional Plant Biology. 2005 May 27;32(5):429-49.

Holtum JA, Hancock LP, Edwards EJ, Winter K. Facultative CAM photosynthesis (crassulacean acid metabolism) in four species of Calandrinia, ephemeral succulents of arid Australia. Photosynthesis Research. 2017 Oct;134(1):17-25.
Google Scholar: Author Only Title Only Author and Title

Holtum JA, Hancock LP, Edwards EJ, Winter K. CAM photosynthesis in desert blooming Cistanthe of the Atacama, Chile. Functional Plant Biology. 2021 Apr 26;48(7):691-702.

Huerta-Cepas J, Szklarczyk D, Forslund K, Cook H, Heller D, Walter MC, Rattei T, Mende DR, Sunagawa S, Kuhn M, Jensen LJ. eggNOG 4.5: a hierarchical orthology framework with improved functional annotations for eukaryotic, prokaryotic and viral sequences. Nucleic acids research. 2016 Jan 4;44(D1):D286-93.

Ignatiadis N, Klaus B, Zaugg JB, Huber W. Data-driven hypothesis weighting increases detection power in genome-scale multiple testing. Nature methods. 2016 Jul;13(7):577-80.
Google Scholar: Author Only Title Only Author and Title

Joyce BL, Haug-Baltzell AK, Hulvey JP, McCarthy F, Devisetty UK, Lyons E. Leveraging CyVerse resources for de novo comparative transcriptomics of underserved (non-model) organisms. Journal of visualized experiments: JoVE. 2017(123).

Karp PD, Midford PE, Billington R, Kothari A, Krummenacker M, Latendresse M, Ong WK, Subhraveti P, Caspi R, Fulcher C, Keseler IM. Pathway Tools version 23.0 update: software for pathway/genome informatics and systems biology. Briefings in bioinformatics. 2021 Jan;22(1):109-26.
Google Scholar: Author Only Title Only Author and Title

Keeley JE, Keeley SC. Crassulacean acid metabolism (CAM) in high elevation tropical cactus. Plant, Cell & Environment. 1989 Apr;12(3):331-6.
Google Scholar: Author Only Title Only Author and Title

Kreslavski VD, Los DA, Schmitt FJ, Zharmukhamedov SK, Kuznetsov VV, Allakhverdiev SI. The impact of the phytochromes on photosynthetic processes. Biochimica et Biophysica Acta (BBA)-Bioenergetics. 2018 May 1;1859(5):400-8.

Krishnakumar V, Contrino S, Cheng CY, Belyaeva I, Ferlanti ES, Miller JR, Vaughn MW, Micklem G, Town CD, Chan AP. ThaleMine: a warehouse for Arabidopsis data integration and discovery. Plant and Cell Physiology. 2017 Jan 1;58(1):e4-.

Lê S, Josse J, Husson F. FactoMineR: an R package for multivariate analysis. Journal of statistical software. 2008 Mar 18;25(1):1-8.

Lim SD, Mayer JA, Yim WC, Cushman JC. Plant tissue succulence engineering improves water-use efficiency, water-deficit stress attenuation and salinity tolerance in Arabidopsis. The Plant Journal. 2020 Aug;103(3):1049-72.
Google Scholar: Author Only Title Only Author and Title

Liu C, Wang H, Zhang X, Ma F, Guo T, Li C. Activation of the ABA Signal Pathway Mediated by GABA Improves the Drought Resistance of Apple Seedlings. International Journal of Molecular Sciences. 2021 Jan;22(23):12676.
Google Scholar: Author Only Title Only Author and Title

Lohse M, Nagel A, Herter T, May P, Schroda M, Zrenner R, Tohge T, Fernie AR, Stitt M, Usadel B. M ercator: a fast and simple web server for genome scale functional annotation of plant sequence data. 2014 May.

López RP, Squeo FA, Armas C, Kelt DA, Gutiérrez JR. Enhanced facilitation at the extreme end of the aridity gradient in the Atacama Desert: a community-level approach. Ecology. 2016 Jun;97(6):1593-604.
Google Scholar: Author Only Title Only Author and Title

Love MI, Huber W, Anders S. Moderated estimation of fold change and dispersion for RNA-seq data with DESeq2. Genome biology. 2014 Dec;15(12):1-21.
Google Scholar: Author Only Title Only Author and Title

Ma Y, Cao J, He J, Chen Q, Li X, Yang Y. Molecular mechanism for the regulation of ABA homeostasis during plant development and stress responses. International journal of molecular sciences. 2018 Nov;19(11):3643.
Google Scholar: Author Only Title Only Author and Title

Maleckova E, Brilhaus D, Wrobel TJ, Weber AP. Transcript and metabolite changes during the early phase of abscisic acid-mediated induction of crassulacean acid metabolism in Talinum triangulare. Journal of experimental botany. 2019 Nov 15;70(22):6581-96.

Males J. Secrets of succulence. Journal of Experimental Botany. 2017 Apr 1;68(9):2121-34.

Martin JA, Wang Z. Next-generation transcriptome assembly. Nature Reviews Genetics. 2011 Oct;12(10):671-82.
Google Scholar: Author Only Title Only Author and Title

Martínez-García JF, Moreno-Romero J. Shedding light on the chromatin changes that modulate shade responses. Physiologia Plantarum. 2020 Jul;169(3):407-17.
Google Scholar: Author Only Title Only Author and Title

Mellenthin M, Ellersiek U, Börger A, Baier M. Expression of the Arabidopsis sigma factor SIG5 is photoreceptor and photosynthesis controlled. Plants. 2014 Sep;3(3):359-91.
Google Scholar: Author Only Title Only Author and Title

Messerschmid TF, Wehling J, Bobon N, Kahmen A, Klak C, Los JA, Nelson DB, dos Santos P, de Vos JM, Kadereit G. Carbon isotope composition of plant photosynthetic tissues reflects a Crassulacean Acid Metabolism (CAM) continuum in the majority of CAM lineages. Perspectives in Plant Ecology, Evolution and Systematics. 2021 Jun 7:125619.
Google Scholar: Author Only Title Only Author and Title

Moseley RC, Motta F, Tuskan GA, Haase SB, Yang X. Inference of gene regulatory network uncovers the linkage between circadian clock and crassulacean acid metabolism in Kalanchoë fedtschenkoi. Cells. 2021 Sep;10(9):2217.
Google Scholar: Author Only Title Only Author and Title

Niechayev NA, Pereira PN, Cushman JC. Understanding trait diversity associated with crassulacean acid metabolism (CAM). Current opinion in plant biology. 2019 Jun 1;49:74-85.

Nielsen SL, Enríquez S, Duarte CM. Control of PAR-saturated CO2 exchange rate in some C3 and CAM plants. Biologia Plantarum. 1997 Jul;40(1):91-101.
Google Scholar: Author Only Title Only Author and Title

Ogburn RM, Edwards EJ. Quantifying succulence: a rapid, physiologically meaningful metric of plant water storage. Plant, Cell & Environment. 2012 Sep;35(9):1533-42.
Google Scholar: Author Only Title Only Author and Title

Osmond CB. Crassulacean acid metabolism: a curiosity in context. Annual Review of Plant Physiology. 1978 Jun;29(1):379-414.
Google Scholar: Author Only Title Only Author and Title

Palma B, Mooney HA. Carbon isotope ratios of Atacama Desert plants reflect hyperaridity of region in northern Chile. Revista Chilena de Historia Natural. 1998;71:79-86.
Google Scholar: Author Only Title Only Author and Title

Parmesan C, Hanley ME. Plants and climate change: complexities and surprises. Annals of botany. 2015 Nov 1;116(6):849-64.

Perdomo JA, Capó-Bauçà S, Carmo-Silva E, Galmés J. Rubisco and rubisco activase play an important role in the biochemical limitations of photosynthesis in rice, wheat, and maize under high temperature and water deficit. Frontiers in plant science. 2017

Apr 13;8:490.

Pereira PN, Cushman JC. Exploring the relationship between crassulacean acid metabolism (CAM) and mineral nutrition with a special focus on nitrogen. International journal of molecular sciences. 2019 Jan;20(18):4363.
Google Scholar: Author Only Title Only Author and Title

Pereira PN, Niechayev NA, Blair BB, Cushman JC. Climate change responses and adaptations in Crassulacean Acid metabolism (CAM) plants. InPhotosynthesis, Respiration, and Climate Change 2021 (pp. 283-329). Springer, Cham.

Poorter H, Niinemets Ü, Poorter L, Wright IJ, Villar R. Causes and consequences of variation in leaf mass per area (LMA): a meta-analysis. New phytologist. 2009 May;182(3):565-88.
Google Scholar: Author Only Title Only Author and Title

Raudvere U, Kolberg L, Kuzmin I, Arak T, Adler P, Peterson H, Vilo J. g: Profiler: a web server for functional enrichment analysis and conversions of gene lists (2019 update). Nucleic acids research. 2019 Jul 2;47(W1):W191-8.

Raven JA, Beardall J. The ins and outs of CO2. Journal of experimental botany. 2016 Jan 1;67(1):1-3.

Raven JA, Beardall J, Sánchez-Baracaldo P. The possible evolution and future of CO2-concentrating mechanisms. Journal of Experimental Botany. 2017 Jun 22;68(14):3701-16.

Schiller K, Bräutigam A. Engineering of Crassulacean Acid Metabolism. Annual review of plant biology. 2021 Jun 17;72:77-103.

Schlaepfer DR, Bradford JB, Lauenroth WK, Munson SM, Tietjen B, Hall SA, Wilson SD, Duniway MC, Jia G, Pyke DA, Lkhagva A. Climate change reduces extent of temperate drylands and intensifies drought in deep soils. Nature communications. 2017 Jan 31;8(1):1-9.

Schläpfer P, Zhang P, Wang C, Kim T, Banf M, Chae L, Dreher K, Chavali AK, Nilo-Poyanco R, Bernard T, Kahn D. Genome-wide prediction of metabolic enzymes, pathways, and gene clusters in plants. Plant physiology. 2017 Apr;173(4):2041-59.
Google Scholar: Author Only Title Only Author and Title

Schweiger AH, Nürk NM, Beckett H, Liede-Schumann S, Midgley GF, Higgins SI. The eco-evolutionary significance of rainfall constancy for facultative CAM photosynthesis. New Phytologist. 2021 May;230(4):1653-64.
Google Scholar: Author Only Title Only Author and Title

Shameer S, Baghalian K, Cheung CM, Ratcliffe RG, Sweetlove LJ. Computational analysis of the productivity potential of CAM. Nature Plants. 2018 Mar;4(3):165-71.
Google Scholar: Author Only Title Only Author and Title

Shelp BJ, Aghdam MS, Flaherty EJ. γ-Aminobutyrate (GABA) Regulated Plant Defense: Mechanisms and Opportunities. Plants. 2021 Sep;10(9):1939.
Google Scholar: Author Only Title Only Author and Title

Simão FA, Waterhouse RM, Ioannidis P, Kriventseva EV, Zdobnov EM. BUSCO: assessing genome assembly and annotation completeness with single-copy orthologs. Bioinformatics. 2015 Oct 1;31(19):3210-2.

Sipes DL, Ting IP. Crassulacean acid metabolism and crassulacean acid metabolism modifications in Peperomia camptotricha. Plant Physiology. 1985 Jan;77(1):59-63.
Google Scholar: Author Only Title Only Author and Title

Smith-Unna R, Boursnell C, Patro R, Hibberd JM, Kelly S. TransRate: reference-free quality assessment of de novo transcriptome assemblies. Genome research. 2016 Aug 1;26(8):1134-44.

Squeo FA. Libro rojo de la flora nativa y de los sitios prioritarios para su conservación: Región de Atacama. 2008. La Serena, Chile: Ediciones de la Universidad de La Serena.

Supek F, Bošnjak M, Škunca N, Šmuc T. REVIGO summarizes and visualizes long lists of gene ontology terms. PloS one. 2011 Jul 18;6(7):e21800.
Google Scholar: Author Only Title Only Author and Title

Töpfer N, Braam T, Shameer S, Ratcliffe RG, Sweetlove LJ. Alternative crassulacean acid metabolism modes provide environment-specific water-saving benefits in a leaf metabolic model. The Plant Cell. 2020 Dec;32(12):3689-705.baud
Google Scholar: Author Only Title Only Author and Title

Vandesompele J, De Preter K, Pattyn F, Poppe B, Van Roy N, De Paepe A, Speleman F. Accurate normalization of real-time quantitative RT-PCR data by geometric averaging of multiple internal control genes. Genome biology. 2002 Jun;3(7):1-2.
Google Scholar: Author Only Title Only Author and Title

Vidiella PE, Armesto JJ, Gutiérrez JR. Vegetation changes and sequential flowering after rain in the southern Atacama Desert. Journal of Arid Environments. 1999 Dec 1;43(4):449-58.

Wai CM, Weise SE, Ozersky P, Mockler TC, Michael TP, VanBuren R. Time of day and network reprogramming during drought induced CAM photosynthesis in Sedum album. PLoS genetics. 2019 Jun 14;15(6):e1008209.
Google Scholar: Author Only Title Only Author and Title

Wang N, Yang Y, Moore MJ, Brockington SF, Walker JF, Brown JW, Liang B, Feng T, Edwards C, Mikenas J, Olivieri J. Evolution of Portulacineae marked by gene tree conflict and gene family expansion associated with adaptation to harsh environments. Molecular biology and evolution. 2019 Jan 1;36(1):112-26.

Wellburn AR. The spectral determination of chlorophylls a and b, as well as total carotenoids, using various solvents with spectrophotometers of different resolution. Journal of plant physiology. 1994 Sep 1;144(3):307-13.

Winter K, Holtum JA. Induction and reversal of crassulacean acid metabolism in Calandrinia polyandra: effects of soil moisture and nutrients. Functional Plant Biology. 2011 Jul 12;38(7):576-82.

Winter K. Ecophysiology of constitutive and facultative CAM photosynthesis. Journal of experimental botany. 2019 Nov 15;70(22):6495-508.

Winter K, Garcia M, Virgo A, Smith JA. Low-level CAM photosynthesis in a succulent-leaved member of the Urticaceae, Pilea peperomioides. Functional Plant Biology. 2020 Dec 8;48(7):683-90.

Winter K, Smith JA. CAM photosynthesis: the acid test. New Phytologist. 2022 Jan;233(2):599-609.
Google Scholar: Author Only Title Only Author and Title

Wright IJ, Reich PB, Westoby M, Ackerly DD, Baruch Z, Bongers F, Cavender-Bares J, Chapin T, Cornelissen JH, Diemer M, Flexas J. The worldwide leaf economics spectrum. Nature. 2004 Apr;428(6985):821-7.
Google Scholar: Author Only Title Only Author and Title

Xu B, Long Y, Feng X, Zhu X, Sai N, Chirkova L, Betts A, Herrmann J, Edwards EJ, Okamoto M, Hedrich R. GABA signalling modulates stomatal opening to enhance plant water use efficiency and drought resilience. Nature communications. 2021 Mar 29;12(1):1-3.

Yang X, Cushman JC, Borland AM, Edwards EJ, Wullschleger SD, Tuskan GA, Owen NA, Griffiths H, Smith JA, De Paoli HC, Weston DJ. 2015. A roadmap for research on crassulacean acid metabolism (CAM) to enhance sustainable food and bioenergy production in a hotter, drier world. New Phytologist 207: 491-504.
Google Scholar: Author Only Title Only Author and Title

Yang Z, Zhang H, Li X, Shen H, Gao J, Hou S, Zhang B, Mayes S, Bennett M, Ma J, Wu C. 2020. A mini foxtail millet with an Arabidopsis-like life cycle as a C4 model system. Nature plants. 6: 1167-1178.
Google Scholar: Author Only Title Only Author and Title

Yang G, Wei Q, Huang H, Xia J. 2020. Amino acid transporters in plant cells: A brief review. Plants. 9: 967.
Google Scholar: Author Only Title Only Author and Title

Yi X, Du Z, Su Z. 2013. PlantGSEA: a gene set enrichment analysis toolkit for plant community. Nucleic acids research 41: W98-103.
Google Scholar: Author Only Title Only Author and Title

Zhang Y, Zhang A, Li X, Lu C. 2020. The role of chloroplast gene expression in plant responses to environmental stress. International Journal of Molecular Sciences 21: 6082.
Google Scholar: Author Only Title Only Author and Title